Modulation of cholera toxin structure and function by host proteins

2014

Helen Burress
University of Central Florida

MODULATION OF CHOLERA TOXIN STRUCTURE AND FUNCTION BY HOST PROTEINS

by

HELEN GISELA BURRESS
B.S. University of Central Florida, 2004
M.S. University of Central Florida, 2010

A dissertation submitted in partial fulfillment of the requirements
for the degree of Doctor of Philosophy
in the Burnett School of Biomedical Sciences
in the College of Graduate Studies
at the University of Central Florida
Orlando, Florida

Summer Term
2014

Major Professor: Kenneth Teter

ABSTRACT

Cholera toxin (CT) moves from the cell surface to the endoplasmic reticulum (ER) where the catalytic CTA1 subunit separates from the holotoxin and unfolds due to its intrinsic thermal instability. Unfolded CTA1 then moves through an ER translocon pore to reach its cytosolic target. Due to the instability of CTA1, it must be actively refolded in the cytosol to achieve the proper conformation for modification of its G protein target. The cytosolic heat shock protein Hsp90 is involved with the ER-to-cytosol translocation of CTA1, yet the mechanistic role of Hsp90 in CTA1 translocation remains unknown. Potential post-translocation roles for Hsp90 in modulating the activity of cytosolic CTA1 are also unknown. Here, we show by isotope-edited Fourier transform infrared (FTIR) spectroscopy that Hsp90 induces a gain-of-structure in disordered CTA1 at physiological temperature. Only the ATP-bound form of Hsp90 interacts with disordered CTA1, and its refolding of CTA1 is dependent upon ATP hydrolysis. In vitro reconstitution of the CTA1 translocation event likewise required ATP hydrolysis by Hsp90. Surface plasmon resonance (SPR) experiments found that Hsp90 does not release CTA1, even after ATP hydrolysis and the return of CTA1 to a folded conformation. The interaction with Hsp90 allowed disordered CTA1 to attain an active state and did not prevent further stimulation of toxin activity by ADP-ribosylation factor 6, a host cofactor for CTA1. This activity is consistent with its role as a chaperone that refolds endogenous cytosolic proteins as part of a foldosome complex consisting of Hsp90, Hop, Hsp40, p23, and Hsc70. A role for Hsc70 in CT intoxication has not yet been established. Here, biophysical, biochemical, and cell-based assays demonstrate Hsp90 and Hsc70 play overlapping roles in the processing of CTA1. Using SPR we determined that Hsp90 and Hsc70 could bind independently to CTA1 at distinct locations with

high affinity, even in the absence of the Hop linker. Studies using isotope-edited FTIR spectroscopy found that, like Hsp90, Hsc70 induces a gain-of-structure in unfolded CTA1. The interaction between CTA1 and Hsc70 is essential for intoxication, as an RNAi-induced loss of the Hsc70 protein generates a toxin-resistant phenotype. Further analysis using isotope-edited FTIR spectroscopy demonstrated that the addition of both Hsc70 and Hsp90 to unfolded CTA1 produced a gain-of-structure above that of the individual chaperones. Our data suggest that CTA1 translocation involves a ratchet mechanism which couples the Hsp90-mediated refolding of CTA1 with extraction from the ER. The subsequent binding of Hsc70 further refolds CTA1 in a manner not previously observed in foldosome complex formation. The interaction of CTA1 with these chaperones is essential to intoxication and this work elucidates details of the intoxication process not previously known.

I would like to dedicate this work to my family, without them, I would have never succeeded. First of all, to my husband, Randy, your support and belief in me has meant the world to me. You have given me great advice, listened to my complaints, and helped me to believe in myself, I love you more every day. To my daughters, thank you for your patience and understanding, when my time was needed for work instead of play. To my mom, thank you for filling in as mom for my family and believing in me along the way. To my dad, I wish you could have been here for this day, but I know that you would have been proud of me. You always told me knowledge is something no one can ever take away from you, and you were right. To my mom-in-law, thank you for being supportive and listening to me vent. And, finally my dad-in-law, I wish you could have been here, but your girl finally finished.

ACKNOWLEDGMENTS

Dr. Teter, thank you for all the support and guidance throughout this process, you are truly a great mentor. To my lab mates, thank you for the help you have given me and for putting up with me. I would also like to thank my committee members for their input and guidance throughout this process. This work was made possible by NIH grant R01AI099493.

TABLE OF CONTENTS

LIST OF FIGURES

LIST OF TABLES

LIST OF ACRONYMS/ABBREVIATIONS

A/A Antibiotic/Antimycotic

ADP Adenosine diphosphate

AHA Activator of Hsp90 ATPase

ARF6 ADP Ribosylation Factor 6

ATP Adenosine triphosphate

ATPγS Adenosine 5'[γ-thio]triphosphate tetralithium salt

BSA Bovine Serum Albumin

CT Cholera Toxin

CTA1 Cholera Toxin A1 subunit

DEA-BAG Diethylamino(benzylidineamino)guanidine

DMEM Dulbecco's modified eagle medium

DTT Dithiolthreitol

EDC 1-ethyl-3-[3-dimethylaminopropyl]carbodiimide hydrochloride

EDTA Ethylenediaminetetraacetic acid

ER Endoplasmic Reticulum

ERAD Endoplasmic Reticulum Associated Degradation

FBS Fetal Bovine Serum

FTIR Fourier Transform Infrared

GA Geldanamycin

GTP Guanosine Tri Phosphate

Hop Hsp Organizing Protein

Hsc70 Heat Shock Cognate 70

Hsp90 Heat Shock Protein 90

IPTG Isopropyl β-D-1-thiogalactopyranoside

K_D Equilibrium dissociation constant

LUV Large Unilamellar Vesicle

mCTA1 Mature Cytosolic CTA1

NAD Nicotinamide Adenine Dinucleotide

NHS N-Hydroxysuccinimide

PBS Phosphate Buffered Saline

PBST Phosphate Buffered Saline with Tween

PIC Protease Inhibitor Cocktail

PVDF Polyvinylidene Difluoride

RIU Refractive Index Unit

SDS Sodium Dodecyl Sulfate

SDS-PAGE Sodium Dodecyl Sulfate Polyacrylamide Gel Electrophoresis

siRNA Small Interfering RNA

SPR Suface Plasmon Resonance

TBST Tris Buffered Saline with Tween

βMe Beta Mercaptoethanol

CHAPTER 1 INTRODUCTION

Cholera Toxin

Cholera toxin (CT) is an AB_5 toxin containing two distinct subunits. The A subunit consists of two domains, A1 and A2, linked by a disulfide bond. The A1 domain is responsible for catalytic activity and the A2 domain acts as a tether between the A1 subunit and the B pentamer. The homopentameric B subunit is a highly stable ring-like structure with a central pore that interacts with the A2 chain and contains binding sites for GM1 gangliosides on the host cell plasma membrane [1, 2].

Binding to GM1 triggers toxin endocytosis from the cell surface and subsequent toxin transport to the endoplasmic reticulum (ER) via retrograde vesicular transport [3, 4]. Reduction of the disulfide bond between the A1 and A2 domains occurs in the ER [5, 6]. Reduced CTA1 is released from its non-covalent association with the holotoxin by protein disulfide isomerase (PDI) [7-9]. The isolated CTA1 domain then enters the cytosol and interacts with host ADP-ribosylation factors (ARFs) to constitutively activate the G protein stimulatory α-subunit (Gsα) through ADP-ribosylation [10-12]. Activation of Gsα increases adenylate cyclase activity, leading to a massive increase in the amount of cAMP produced. The increased level of cAMP stimulates Cl^- release and inhibits Na^+ absorption in intestinal epithelial cells, causing an efflux of water that generates the profuse watery diarrhea associated with cholera [2, 13].

ER Associated Degradation

The isolated CTA1 polypeptide is an unstable protein that assumes a disordered conformation at physiological temperature [14]. The conformational instability of free CTA1 affects many steps of the intoxication process [15, 16]. For example, CTA1 spontaneously unfolds after its PDI-mediated release from the holotoxin in the ER [8]. Unfolded CTA1 is then exported to the cytosol through the ER-associated degradation (ERAD) pathway [17-22]. The ER to cytosol translocation of unfolded proteins by ERAD is a normal process that prevents the accumulation of protein aggregates the ER. Exported ERAD substrates move through protein-conducting channels in the ER membrane and are targeted for cytosolic degradation by the 26S proteasome in an ubiquitin-dependent manner [23, 24]. A number of AB toxins exploit this system for A chain passage into the cytosol [15, 25, 26].

Proteasomal Degradation

CTA1 and other toxin A chains contain an arginine-over-lysine bias in its amino acid sequence. The lack of CTA1 lysine residues limits the number of ubiquitination sites, thereby inhibiting toxin degradation by the 26S proteasome [25, 27, 28]. CTA1 is still subject to ubiquitin-independent degradation by the core 20S proteasome [14], a variant of the proteasome that can only degrade unfolded proteins [29]. The relatively long half-life ($t_{1/2}$ = 2 hours) for cytosolic CTA1 suggests a stabilizing interaction with host factors may protect CTA1 from rapid, ubiquitin-independent proteasomal degradation [14].

Translocation

CTA1 instability also plays a role in toxin extraction from the ER to the cytosol. An early model of toxin translocation proposed CTA1 spontaneously refolded as it emerged at the cytosolic face of the ER translocon pore [27]. This would prevent backsliding in the pore and would thereby provide an ER-to-cytosol directionality to the translocation process. Yet the subsequent discovery of CTA1 conformational instability indicated that the toxin could not independently refold at physiological temperature and therefore required a host factor(s) for extraction to the cytosol [14, 30]. While most ERAD export is mediated by the AAA ATPase, p97 [31, 32], CTA1 translocation does not require this cytosolic protein [33, 34]. The ER-to-cytosol translocation of unfolded CTA1 is instead facilitated by heat shock protein 90 (Hsp90), a cytosolic ATP-dependent chaperone that plays a role in multiple cellular events including protein folding, protein stabilization, and refolding of denatured proteins [35, 36]. Loss of Hsp90 function has shown that CTA1 is trapped in the ER [37].

Activity

CTA1 passes through one or more ER translocon pores [38-40] in an unfolded state and must achieve an active conformation in the cytosol to modify its G protein target in the lipid rafts of the plasma membrane [41-45]. Refolding will not occur spontaneously because CTA1 is a thermally unstable protein. In fact, the isolated CTA1 polypeptide has little to no enzymatic activity at 37°C [46, 47]. An interaction with ARF proteins will enhance the activity of folded CTA1 and is required for productive intoxication of cultured cells, but ARF alone cannot induce a gain-of-structure or gain-of-function in disordered CTA1 (Banerjee, submitted manuscript).

Other host factors must therefore place cytosolic CTA1 in a folded conformation that can be further activated by ARF proteins. Lipid rafts were recently shown to exhibit a "lipochaperone" property that places disordered CTA1 in a folded, functional state at physiological temperature. Furthermore, lipid rafts are essential for the in vivo activity of cytosolic CTA1 [46]. However, other host factors that could refold and/or activate cytosolic CTA1 have yet to be identified.

CHAPTER 2 MATERIALS AND METHODS

Materials

Chemicals and Reagents

Sigma (St. Louis, Missouri)
100X Vitamin Solution
Adenosine Tri-Phosphate (ATP)
Aminoguanidine bicarbonate
Boric acid (H_3BO_3)
Copper chloride ($CuCl_2$)
Digitonin
Dithiolthreitol (DTT)
DNAse
Guanosine Tri-Phosphate (GTP)
HEPES
Iron chloride ($FeCl_2$)
Magnesium Sulfate ($MgSO_4$)
Niaproof 40 (NP40)
Nα', Nα-Bis(carboxymethyl)-L-lysine hydrate
Potassium chloride (KCl)
Protease inhibitor cocktail for His proteins (His-PIC)
Sodium molybdate (Na_2MoO_4)
Sodium tetraborate ($Na_2B_4O_7$)

Santa Cruz (Dallas, TX)
4-Diethylaminobenzaldehyde

Enzo Life Sciences (Farmingdale, NY)
Adenosine 5'[γ-thio]triphosphate tetralithium salt (ATPγS)

Fisher Scientific (Pittsburgh, PA)
1-ethyl-3-[3-dimethylaminopropyl]carbodiimide hydrochloride (EDC)
Ammonium chloride (NH_4Cl_2)
Ammonium sulfate ($(NH_4)_2SO_4$)
Ampicillin
Calcium chloride ($CaCl_2$)
Coomassie R-250
Deoxycholic Acid

Disodium phosphate (Na_2HPO_4)
Ethanol (200 proof)
Ethylenediaminetetraacetic acid (EDTA)
Glycerol
Hydrochloric Acid (HCl)
Imidazole
Luminol
Magnesium Chloride ($MgCl_2$)
Methanol
N-Hydroxysuccinimide (NHS)
Potassium phosphate (KH_2PO_4)
Sodium Acetate (NaOAc)
Sodium Chloride (NaCl)
Sodium Hydroxide (NaOH)
Tris Base
Tryptone
Tween 20
Urea
Yeast extract
β-mercaptoethanol (BME)

Medicago (Research Triangle Park, NC)
Phosphate Buffered Saline with 0.05% Tween Tablets (PBST)

Qiagen (Venlo, Limburg)
Qiagen Miniprep kit

Perkin Elmer (Waltham, MA)
^{35}S-labeled methionine

Cambridge Isotope (Tewksbury, MA)
^{13}C-labeled $^{13}C_6$-D-glucose

VWR International (Radnor, PA)
Isopropyl β-D-1-thiogalactopyranoside (IPTG)
Nicotinamide adenine dinucleotide (NAD)

Amresco (Solon, OH)
Triton X-100
PVDF membrane

MP Biologicals (Illkrich, France)
Cobalt chloride ($CoCl_2$)
Coumaric acid

Hoefer (San Francisco, CA)
Sodium dodecyl sulfate (SDS)

Acros (Geel, Belgium)
Mangenese chloride ($MnCl_2$)
Nickel sulfate ($NiSO_4$)

Antibodies

Santa Cruz (Dallas, TX)
Anti-ARF6 rabbit polyclonal

Calbiochem (Darmstadt, Germany)
Anti-Hsp90 rabbit polyclonal

Sigma (St. Louis, MO)
Anti-Cholera toxin rabbit polyclonal
Anti-Hsp40 rabbit polyclonal

Enzo Life Sciences (Farmingdale, NY)
Anti-Hsp40 rabbit polyclonal
Anti-Hop rabbit polyclonal

Abcam (Cambridge, England)
Anti-Hsp90 rabbit polyclonal
Anti-Hsc70 rat monoclonal

Jackson ImmunoResearch (West Grove, PA)
Goat anti-Rabbit secondary HRP conjugate

Proteins

Biovision (Milpitas, CA)
Heat shock protein 90 (Hsp90)

Abcam (Cambridge, England)
Hsc70

Boston Biochem (Cambridge, MA)
20S Proteasome

26S Proteasome

Enzo Life Sciences (Farmingdale, NY)
AHA
Hop
p23

Toxins

Sigma (St. Louis, MO)
Cholera Toxin (CT)
Cholera Toxin A1/A2 (CTA1/2)

List Biologicals (Campbell, CA)
Cholera Toxin A1/A2 (CTA1/2)

Tissue Culture Reagents

Invitrogen (Carlsbad, CA)
Antibiotic/Antimycotic (A/A)
Dulbecco's modified eagle medium (DMEM)
Ham's F-12 Medium
Lipofectamine
OPTIMEM

Atlanta Biologicals (Flowery Branch, GA)
Fetal Bovine Serum (FBS)

Other Materials

Clontech (Mountain View, CA)
Talon Resin

GE Healthcare (Piscataway, NJ)
DEAE ion exchange column

Biorad (Hercules, CA)
AG50W-4X beads

Buffers

10X Phosphate Buffered Saline (PBS)
82.3 g Na_2HPO_4 (0.58M)
23.5 g NaH_2PO_4 (0.17M)
40.0 g NaCl (0.69 M)
H_2O to 1 L and autoclave

10X Tris Buffered Saline (TBS)
24.24 g Tris Cl pH 7.5
5.56 g Tris Base
80.1g NaCl
H_2O to 1 L

10X Tris Buffered Saline with Tween (TBST)
24.24 g Tris Cl pH 7.5
5.56 g Tris Base
80.1g NaCl
10 ml Tween20
H_2O to 1 L

10X SDS PAGE Running Buffer (RB)
30.2 g Tris Base
144 g Glycine
10 g SDS
H_2O to 1 L

Transfer Buffer
100 ml 10X Running buffer
200 ml 100% Methanol
700 ml H_2O

HCN Buffer
50 mM HEPES pH 7.5
150 mM NaCl
2mM $CaCl_2$
10 mM N-ethylmaleimide
10 µl/ml PIC

Lysis Buffer
25 mM Tris-Cl pH 7.4
20 mM NaCl
1% Deoxycholic Acid
1% Triton X-100

10 µl/ml PIC

Lysine Hydrate Buffer (His-tag Immobilization)
0.15 M $N_{\alpha'}$-N_{α}-Bis carboxymethyl-L-Lysine Hydrate in 20mM Sodium Acetate (pH 5.2)-filter

0.1 M Sodium Phosphate Buffer
195 ml 0.2M NaH_2PO_4
305 ml 0.2M Na_2HPO_4
500 ml H_2O

Digitonin Buffer
2.5 mg digitonin dissolved in 250 µl warmed 200 proof ethanol
Add 40 µl digitonin/ethanol to 960 µl HCN buffer

Borate Buffer
10 mM Sodium borate
100 mM NaCl

Solutions

5X M9 salts
64 g Na_2HPO_4 $7H_2O$
15 g KH_2PO_4
2.5 g NaCl
H_2O to 1L and Autoclave

Solution Q
8 ml 5M HCl
5 g $FeCl_2$
185 mg $CaCl_2$
64 mg H_3BO_3
18 mg $CoCl_2$
4 mg $CuCl_2$
605 mg Na_2MoO_4
40 mg $MnCl_2$ $4H_2O$
H_2O to 1 L and filter sterilize

M9 Minimal Media
100 ml 5X M9 salts
1 ml 1M $MgSO_4$
50 µl 1M $CaCl_2$
5 ml 100X Vitamin Solution

2 ml Solution Q
5 ml Filter sterilized 0.1 g/ml NH_4Cl
5 ml Filter sterilized 0.1 g/ml $(NH_4)_2SO_4$
2 g dry $^{13}C_6$-D-glucose
Autoclaved H_2O to 500 ml

Luria Bertani Media
10 g Tryptone
5 g Yeast extract
5 g NaCl
H_2O to 1 L and autoclave

NDET
1% NP-40
0.4% Deoxycholic Acid
5 mM EDTA
10 mM Tris-Cl, pH 7.4
150 mM NaCl

Coomassie Stain
1.0 g Coomassie Brilliant Blue R-250
50 ml Glacial Acetic Acid
500 ml Methanol
450 ml dH20

Coomassie Destain
10% Glacial Acetic Acid
50% Methanol

ECL Developing Solution Stock
1 ml 250 mM Luminol
444 ul 90 mM ρ-coumaric acid
10 ml 1 M Tris pH 8.5
Water to 100 mL

ECL Working Solution
5 ml ECL developing solution stock
5 ml 100 mM Tris pH 8.5
3.1 µl 30% hydrogen peroxide

Methods

Purification of CTA1-His_6

5 ml Luria Bertani (LB) media containing 100 μg/ml ampicillin was inoculated with *Escherichia coli* strain BL21 pLysS transformed with pT7CTA1h6, an inducible CTA1-His_6 expression plasmid, and grown at 37°C overnight with shaking. The culture was then expanded to 1000 ml LB media containing 100 μg/ml ampicillin, incubated at 37°C with shaking, and allowed to reach OD_{600} of 0.6-0.8. The culture was then induced with 1mM IPTG for 18 h at 18°C. The cells were then centrifuged at 6000 rpm and 4°C for 20 minutes. The supernatant was discarded, and the cells were resuspended in extraction buffer containing 20 mM Tris-HCl pH 7.0, 300 mM NaCl, 8 M urea, 0.1% sodium deoxycholate, 100 μg/ml lysozyme and 0.1 μl/ml DNAse. Following three freeze/thaw cycles at -80°C /37°C, the lysed cells were centrifuged at 12000 rpm for 30 min at 4°C. The supernatant was collected, syringe filtered to remove any remaining cellular debris and 10 μl/ml His-PIC was added. For every 5 ml of crude lysate, 1 ml Talon resin beads were prepared as described by the manufacturer. After equilibration of the resin with extraction buffer, lysate was added to the resin and agitated at room temperature for 45 min. The resin was then centrifuged at 700 g for 5 min, and the supernatant was removed and labeled as unbound lysate. The resin with bound proteins was then resuspended with wash buffer containing 20 mM Tris-HCl pH 7.0, 600 mM NaCl and 0.1% Triton X-100 and agitated at room temperature for 15 min. The resin was centrifuged at 700 g for 5 minutes and the supernatant removed and labeled as wash. Washes were repeated twice. The washed beads were then resuspended in buffer, transferred to a gravity flow column and allowed to settle. The resin bed

was then washed with buffer, and the wash was collected and saved. CTA1-His_6 was then eluted from the column using 2 mL of increasing concentrations of imidazole (10, 15, 20, 25, 35, 40, and 50 mM), with 0.5 ml fractions collected. Fractions were stored at 4°C until needed. Samples of each step and elution fractions were prepared for SDS-PAGE and Coomassie staining for verification of purity. Prior to use, samples were dialyzed in 20 mM sodium phosphate (pH 7.0) buffer containing 6 M urea for 2 h at room temperature, 4 M urea overnight at 4°C, 2 M urea for 2 h at 4°C, urea-free buffer for 1 h at 4°C followed by another urea-free buffer for 30 min at 4°C. Dialyzed samples were used within 24 h.

^{13}C Labeling and Purification of CTA1-His_6

5 ml M9 minimal media containing 100 μg/ml ampicillin was inoculated with *E. coli* strain BL21 pLysS transformed with pT7CTA1h6, an inducible CTA1-His_6 expression plasmid, and grown at 37°C overnight with shaking. The culture was then expanded to 1000 ml M9 minimal media supplemented with ^{13}C-labeled $^{13}C_6$-D-glucose containing 100 μg/ml ampicillin, incubated at 37°C with shaking and allowed to reach OD_{600} of 0.6-0.8. The culture was then induced with 1 mM IPTG for 18 h at 18°C. The cells were then centrifuged at 6000 rpm 4°C for 20 min. The supernatant was discarded, and the cells were resuspended in extraction buffer containing 20 mM Tris-HCl pH 7.0, 300 mM NaCl, 8 M urea, 0.1% sodium deoxycholate, 100 μg/ml lysozyme and 0.1 μl/ml DNAse. Following three freeze/thaw cycles at -80°C /37°C, the lysed cells were centrifuged at 12000 rpm for 30 min at 4°C. The supernatant was collected, syringe filtered to remove any remaining cellular debris and 10 μl/ml His-PIC was added. For every 5 ml of crude lysate, 1 ml Talon resin beads were prepared as described by the manufacturer. After

equilibration of the resin with extraction buffer, lysate was added to the resin and agitated at room temperature for 45 min. The resin was then centrifuged at 700 g for 5 min, and the supernatant was removed and labeled as unbound lysate. The resin with bound proteins was then resuspended with wash buffer containing 20 mM Tris-HCl pH 7.0, 600 mM NaCl and 0.1% Triton X-100 and agitated at room temperature for 15 min. The resin was centrifuged at 700 g for 5 min, and the supernatant was removed and labeled as wash. Washes were repeated twice. The washed beads were then resuspended in buffer, transferred to a gravity flow column and allowed to settle. The resin bed was then washed with buffer, and the wash was collected and saved. CTA1-His_6 was then eluted from the column using 2 ml of increasing concentrations of imidazole (10, 15, 20, 25, 35, 40, and 50 mM), with 0.5 ml fractions collected. Fractions were stored at 4°C until needed. Samples of each step and elution fractions were prepared for SDS-PAGE and Coomassie staining for verification of purity. Prior to use, samples were dialyzed in 20 mM sodium borate buffer (pH 7.0) containing 100 mM NaCl to facilitate refolding. Samples were dialyzed in borate buffer containing 6 M urea for 2 h at 4°C, 2 M urea for 2 h at 4°C, 1M urea for 2 h at 4°C, urea-free buffer for 2 h at 4°C followed by another urea-free buffer for 2 h at 4°C. Dialyzed samples were then lyophilized and stored at -80°C.

Isotope Edited Fourier Transform Infrared Spectroscopy

Samples for FTIR measurement (^{13}C labeled CTA1-His_6, Hsp90, Hsc70, ATP, and ATPγS) were prepared in D_2O-based 10 mM sodium borate buffer (pD 7.0) containing 100 mM NaCl. A 2:1 molar ratio of Hsp90:CTA1 and a 1:1 molar ratio of Hsc70:CTA1 was used for all measurements. Spectra were collected using a Jasco 4200 FTIR spectrometer (Easton, MD) with

the spectral resolution set at 0.964 cm^{-1} and a set resolution of 1 cm^{-1}. Uniformly ^{13}C-labeled CTA1 was used in order to shift the spectra of the labeled protein approximately 45 cm^{-1} from unlabeled Hsp90 and Hsc70. The ^{13}C-labeled protein was assigned wavenumbers corresponding to protein secondary structures in the amide I region: α-helix (1600-08 cm^{-1}), β-sheet (1570-84 cm^{-1}), irregular (1588-98 cm^{-1}), and turns (1610-18 cm^{-1}). Deconvolution of protein secondary structures was performed using Grams/AI software (ThermoScientific, San Francisco, CA).

Purification of ARF6

E. coli strain BL21 pLysS carrying an expression plasmid for ARF6 was grown at 37°C in Luria-Bertani media and induced at OD_{600} 0.6-0.8 by adding 1 mM IPTG. After overnight induction at 18°C, the cells were pelleted and resuspended in buffer containing 20 mM Tris (pH 8.0), 100 mM NaCl, 1 mM DTT, 2 mM EDTA and 1 mM $MgCl_2$. The resuspended cells were lysed using three -80°C /37°C freeze thaw cycles and then centrifuged at 16,200 g for 30 min. The supernatant was dialyzed in buffer containing 20 mM Tris (pH 7.6), 50 mM NaCl, 1 mM DTT, 2 mM EDTA and 1 mM $MgCl_2$ with two exchanges for 2 h each. The dialyzed lysate was then passed through a 0.45 µm pore syringe filter prior to loading it on a DEAE ion exchange column. The column was equilibrated using buffer containing 20 mM Tris (pH 7.6) and 50 mM NaCl before use. Samples were collected in 1 ml fractions and were run on a 15% gel to check for purity. Samples were verified by immunoblot using an ARF6 specific antibody.

Diethylamino(benzylidineamino)guanidine (DEA-BAG) Synthesis

500 ml of 0.11 M aminoguanidine bicarbonate pH 6.5 was filtered to remove insoluble solids and heated to 60°C. 9.74 g 4-Diethylaminobenzaldehyde added to make a 1:1 molar ratio to the aminoguanidine bicarbonate. After removing from heat, approximately 300 ml of 200 proof ethanol was added to make the solution homogenous. The solution was stirred at room temperature for 16 h. Existing precipitate was harvested by filtration, and the remaining mixture was evaporated and cooled to promote further precipitate formation. Collected precipitate was then lyophilized and stored at -80°C.

In Vitro ADP-Ribosylation Assay

To monitor the catalytic activity of CTA1, the stated concentrations of CTA1-His_6 were placed in 200 µl assay buffer containing 200 mM potassium phosphate buffer (pH 7.5), 20 mM DTT, and 0.1 mg/ml BSA. Hsp90 at a 2:1 molar ratio to CTA1, equimolar ARF6, and/or 800 µM lipid raft LUVs were also present as indicated, as were 1 mM ATP, ATPγS, or GTP. CTA1 samples were incubated for 30 min at 25°C or 37°C, followed by addition of the indicated components and further incubation for 1 h at respective temperature followed by addition of 0.4 mg DEA-BAG. For experiments dependent upon sequential addition of components, following the 30 min pre-incubation of CTA1, the first set of host factor(s) was added and allowed to incubate at the indicated temperature for 1 h. Following this incubation, the second set of host factor(s) was added and incubated for another hour at the indicated temperature. The ADP-ribosylation reaction was initiated by addition of 25 µl 10 mM NAD, and samples were incubated at the indicated temperature for two hours during which CTA1, if active, was able to ADP-ribosylate

the artificial substrate (DEA-BAG). The reaction was stopped by addition of 800 µl of 30% AG50W-4X bead slurry. ADP-ribosylation of DEA-BAG inhibits its ability to bind to AG50W-4X beads, so the resulting supernatant contains only modified substrate. The samples were vortexed for 30 sec, followed by centrifugation at maximum speed for 10 min. 400 µl of supernatant was removed and fluorescence (excitation 361 nm, emission 440 nm) was read by Bio-Tek Synergy 2 plate reader (Winooski, VT).

Cell Culture and Transfection

CHO cells were seeded to 6-well plates in Ham's F-12 media supplemented with 10% fetal bovine serum and incubated overnight at 37°C with 5% CO_2 to reach 60-80% confluency. Cells were washed two times with OPTIMEM, and 0.8 ml of OPTIMEM was added to each well. Lipofectamine was diluted in OPTIMEM at a ratio of 1:20 and incubated for 5 min at room temperature. A plasmid encoding the mature CTA1 polypeptide (pcDNA3.1/mCTA1) was diluted at a ratio of 1 µg DNA:100 µl OPTIMEM and incubated for 5 min at room temperature. The diluted plasmid and lipofectamine mixtures were then combined and allowed to incubate at room temperature for 30 min. 200 µl of the mixture was then added to each well and incubated at 37°C and 5% CO_2 for 3 h. At the end of the transfection, cells were rinsed with Ham's F-12 media and incubated in 1 ml Ham's F-12 media at 37°C and 5% CO_2 for 4 h (to monitor cAMP levels) or overnight (to monitor the turnover of CTA1).

Metabolic Labeling and Immunoprecipitation

CHO cells transfected with pcDNA3.1/mCTA1were incubated for 30 min at 37 °C and 5% CO_2 with methionine-free DMEM. The cells were then incubated with methionine-free DMEM supplemented with 150 μCi/ml ^{35}S-labeled methionine. A subset of intoxicated cells was also incubated with 0.1 μM of the Hsp90 inhibitor geldanamycin (GA). All cells were then chased for 0-4 h in radiolabel-free medium either lacking or containing 0.1 μM GA. After each stated chase point, clarified cell extracts generated from a 20 min 4°C exposure to lysis buffer (25 mM Tris-Cl (pH 7.4), 20 mM NaCl, 1% deoxycholic acid, 1% Triton X-100, protease inhibitor cocktail) were incubated overnight at 4°C with sepharose A beads conjugated with an anti-CT antibody. After centrifugation at 2000 rpm for 5 min, the supernatant was removed and beads were rinsed twice with NDET (1% NP-40, 0.4% deoxycholic acid, 5 mM EDTA, 10 mM Tris-Cl (pH 7.4), 150 mM NaCl) and once with water before the addition of 1X sample buffer. Samples boiled for 5 min were resolved by sodium dodecyl sulfate polyacrylamide gel electrophoresis (SDS-PAGE) on 15% polyacrylamide gels and visualized by Biorad Personal Molecular Imager (Hercules, CA), and the image was processed using Biorad Quantity One software. Background pixel intensity was subtracted from each lane; each value was set as a percentage of the 0 h value.

Surface Plasmon Resonance (SPR) Nickel NTA sensor slides

Experiments were performed with a Reichert (Depew, NY) SR7000 SPR refractometer. To capture His-tagged CTA1 on nickel-NTA sensor slides, a Reichert SPR sensor slide with a mixed self-assembled monolayer was rinsed with 2 M NaCl and 10 mM NaOH. The slide was

then rinsed with water and activated with 0.08 mg/ml 1-ethyl-3-[3-dimethylaminopropyl] carbodiimide hydrochloride (EDC) and 0.02 mg/ml N-Hydroxysuccinimide (NHS) for 10 min. The slide was then rinsed with water again and covered with 1 mg/ml Nα', Nα-Bis(carboxymethyl)-L-lysine hydrate in 20 mM sodium acetate (pH 5.2). After an overnight incubation, the slide was rinsed with water and covered with 1 M ethanolamine (pH 8.5) for 10 min. The slide was then rinsed with water and allowed to dry. After mounting the activated slide in the SPR instrument, 0.01 M phosphate buffered saline (pH 7.4) with 0.05% Tween® 20 (PBST) was perfused over the plate. An injection of 40 mM nickel sulfate was then perfused over the plate for 5 min. His-tagged CTA1 diluted in 20 mM sodium acetate (pH 5.5) was then perfused over the plate for 5 min followed by PBST for 5-10 min. After establishment of a new baseline measurement corresponding to the mass of the sensor-bound CTA1, Hsp90, Hsc70, ARF6, or other ligands were perfused over the CTA1-coated sensor slide. Protein concentration was 1600 ng/ml in PBST unless otherwise noted. A 5 min perfusion of ligand was followed by a 5 min PBST wash. The flow rate for all steps was 41 µl/min. Reichert Labview software was used for data collection. The BioLogic (Campbell, Australia) Scrubber 2 software and WaveMetrics (Lake Oswego, OR) Igor Pro software were used to analyze the data and generate figures.

Surface Plasmon Resonance (SPR) Antibody Coated sensor slides

Experiments were performed with a Reichert SR7000 SPR refractometer. To capture proteins on antibody-coated sensor slides, a Reichert SPR sensor slide with a mixed self-assembled monolayer was mounted in the SPR instrument, and PBST was perfused over the plate. The

plate was then activated with 0.08 mg/ml EDC and 0.02 mg/ml NHS for 5 min. The slide was then rinsed with a perfusion of PBST for 5 min. The antibody of interest was diluted in 20 mM sodium acetate (pH 5.5) and then perfused over the plate for 5 min followed by PBST for 5 min. The activated plate was then blocked by a 5 min perfusion of 1 M ethanolamine (pH 8.5) followed by PBST for 5-10 min. After establishment of a new baseline measurement corresponding to the mass of the sensor-bound antibody, ligands were perfused over the antibody-coated sensor slide. Protein concentration was 1600 ng/ml in PBST unless otherwise noted. A 5 min perfusion of ligand was followed by a 5 min PBST wash. The flow rate for all steps was 41 µl/min. Reichert Labview software was used for data collection. The BioLogic (Campbell, Australia) Scrubber 2 software and WaveMetrics (Lake Oswego, OR) Igor Pro software were used to analyze the data and generate figures.

Surface Plasmon Resonance (SPR) Amine Coupled sensor slides

Experiments were performed with a Reichert SR7000 SPR refractometer. To directly couple a protein to a sensor slide, a Reichert SPR sensor slide with a mixed self-assembled monolayer was mounted in the SPR instrument, and PBST was perfused over the plate. The plate was then activated with 0.08 mg/ml EDC and 0.02 mg/ml NHS for 5 min. The slide was then rinsed with a perfusion of PBST for 5 min. The protein of interest was diluted in 20 mM sodium acetate (pH 5.5) and then perfused over the plate for 5 min followed by PBST for 5 min. The activated plate was then blocked by a 5 min perfusion of 1 M ethanolamine (pH 8.5) followed by PBST for 5-10 min. After establishment of a new baseline measurement corresponding to the mass of the sensor-bound protein, the ligand(s) of interest was perfused over the protein-coated sensor slide.

Protein concentration was 1600 ng/ml in PBST unless otherwise noted. A 5 min perfusion of ligand was followed by a 5 min PBST wash. The flow rate for all steps was 41 µl/min. Reichert Labview software was used for data collection. The BioLogic (Campbell, Australia) Scrubber 2 software and WaveMetrics (Lake Oswego, OR) Igor Pro software were used to analyze the data and generate figures.

Western Blot

Following transfer of protein to PVDF membrane, the membrane was washed briefly in TBST. The TBST was removed and replaced with 5% dry milk/TBST solution for 10 min rocking to block unbound membrane. The blocking solution was then removed and replaced with primary antibody diluted in 1% dry milk/TBST solution at the indicated ratio. The membrane was incubated with rocking at 4°C overnight. The primary antibody solution was removed, and the membrane was washed four times with 1% milk/TBST and rocking for 15 min each wash. The solution was then replaced with secondary antibody (goat anti-rabbit HRP) at a dilution of 1:10000 in 1% milk/TBST solution. The membrane was incubated for 30 min at room temperature with rocking. The secondary antibody was then removed and the membrane was washed twice with milk/TBST with rocking for 15 min each. The membrane was then washed with TBST with rocking for 15 min and repeated. After removal of the TBST, ECL developing solution was added for 5 min with rocking at room temperature. The membrane was then transferred to cassette for exposure. Primary antibodies dilutions were as follows: anti-Hsp90 1:5000, anti-CT 1:10000, anti-Hsc70 1:5000.

Digitonin Permeabilization

CHO cells were seeded to 6 well plates in Ham's F-12 media supplemented with 10% fetal bovine serum and incubated overnight at 37°C with 5% CO_2 to reach 60-70% confluency. Cells were washed two times with F-12 media and incubated overnight at 37°C with 5% CO_2. Cells were then washed two times with PBS, and 1 ml of PBS with 0.5 mM EDTA was added for 5-10 min incubation. 3 wells of cells per condition were then transferred to microcentrifuge tubes and centrifuged at 5000 g for 2 min. PBS was removed, and cells and digitonin buffer (0.04% digitonin in HCN buffer with 10 µl/ml PIC) were allowed to incubate separately on ice for 10 min. Following incubation, 100 µl of digitonin buffer was added to each sample for exactly 10 min. The samples were then centrifuged at 14000 g for 10 min. The supernatant (containing cytosolic components) and pellet (containing membrane bound components) were then separated and stored at -20 °C until needed.

In Vitro Translocation Assay

CHO cells were seeded to 6 well plates in Ham's F-12 media supplemented with 10% fetal bovine serum and incubated overnight at 37°C with 5% CO_2 to reach 60-70% confluency. Cells were washed two times with F-12 media, and 1 ml of 100 ng/ml CT was added to each well. Cells were then incubated 2 h at 37°C with 5% CO_2. Cells were then washed two times with PBS, and 0.5 ml of PBS with 0.5 mM EDTA was added for a 5-10 min incubation at room temperature. 3 wells of cells per condition were then collected in a microcentrifuge tube and centrifuged at 5000 g for 2 min. PBS was removed, and cells and digitonin buffer (0.04% digitonin in HCN buffer with 10 µl/ml PIC) were allowed to incubate separately on ice for 10

min. Following this pre-incubation, 100 µl of digitonin buffer was added to each sample for 10 min. The samples were then centrifuged at 13000 rpm for 10 min. The supernatant, containing cytosolic components, and pellet, containing membrane bound components, were separated for further processing. Pelleted membranes were then incubated with 800 mM NaCl in PBS for 30 min at 4°C to remove membrane associated proteins. The pellet was then washed two times with PBS followed by 5 min centrifugation at 13000 rpm. Wash buffer was removed, and excess purified Hsp90, ATP, Hsp90/ATP, or Hsp90/ATPγS in HCN buffer was then added to the membrane fraction and incubated for 1 h at 4°C. After a 5 min spin at 13000 g, the supernatant was collected and perfused over an anti-CTA coated sensor slide. Verification of the fidelity of membrane stripping was performed via Western blotting. 20 µl of sample was loaded on a 15% gel and separated by SDS-PAGE. The gel was transferred to PVDF membrane, and Western blotting was performed with rabbit anti-Hsp90 at a dilution of 1:5000.

CHAPTER 3 CO-AND POST-TRANSLOCATION ROLES FOR HSP90 IN CHOLERA INTOXICATION

Introduction

The high affinity interaction between CTA1 and Hsp90 [37], combined with the established chaperone activity of Hsp90, suggests Hsp90 could be another host factor linked to the cytosolic activity of CTA1.

To provide molecular detail regarding the co- and post-translocation roles of Hsp90 in CT intoxication, we performed a structure-function analysis on the interaction between Hsp90 and CTA1. Biophysical measurements provided a mechanistic basis for Hsp90-mediated extraction of CTA1 from the ER by demonstrating that Hsp90 can convert disordered CTA1 to a structured conformation. ATP hydrolysis was required for Hsp90 to refold CTA1 and to maintain a high-affinity interaction with the refolded toxin. ATP hydrolysis by Hsp90 was also required for the ER-to-cytosol export of CTA1. The Hsp90-mediated refolding of CTA1 thus appears to provide the driving force for toxin extraction from the ER. Hsp90 remained associated with the refolded toxin and did not release CTA1 upon exposure to a number of host factors known to interact with Hsp90 and/or CTA1. The continued association of CTA1 with Hsp90 did not protect the toxin from proteasomal degradation. The interaction with Hsp90 did not interfere with the ability of CTA1 to manifest its enzymatic activity at physiological temperature. This basal level of in vitro toxin activity could be further enhanced by ARF6 and lipid rafts. However, the toxin had to be incubated with Hsp90 and ARF6 before exposure to lipid rafts; simultaneous treatment with Hsp90, ARF6, and lipid rafts at 37°C actually inhibited toxin activity. Our studies suggest CTA1

translocation involves a ratchet mechanism which couples the Hsp90-mediated refolding of CTA1 with CTA1 extraction from the ER. Continued association of Hsp90 with refolded CTA1 allows the cytosolic toxin to attain an active conformation but does not protect it from proteasomal degradation. Our data thus provides mechanistic insight into how Hsp90 modulates the structure and function of CTA1.

Hsp90 refolds disordered CTA1 in a process requiring ATP hydrolysis

Isotope-edited Fourier transform infrared spectroscopy (FTIR) was performed to examine the effect of Hsp90 on the folding state of CTA1 (Fig. 1). Uniformly ^{13}C-labeled CTA1 was used in order to differentiate between the spectra of CTA1 and unlabeled Hsp90. An approximately 45 cm^{-1} shift in the spectra of the ^{13}C-labeled protein allows it to be resolved from the spectra of the unlabeled protein thus facilitating analysis of the individual proteins [8, 48]. The spectra of CTA1 alone (Fig. 1A) showed that, at 10°C, CTA1 is in a folded conformation with approximately 34% α-helical, 42% β-sheet, and 17% irregular (i.e. undefined) structure (Table 1). The amount of secondary and irregular structure in CTA1 at 10°C was consistent with previous FTIR measurements of folded CTA1 [8] and the structural content of holotoxin-associated CTA1 determined by X-ray crystallography [1, 49]. As expected from the intrinsic instability of CTA1, increasing the temperature to 37°C caused CTA1 to unfold: it lost at least half of its initial α-helical and β-sheet content, while the amount of irregular structure increased to 54% (Fig. 1B, Table 1). In the absence of ATP, Hsp90 cannot bind to CTA1 [37] and accordingly had no appreciable effect on the structure of CTA1 when added to the unfolded toxin at 37°C (Fig. 1C, Table 1). However, the addition of Hsp90/ATP to unfolded CTA1 at

37°C produced a substantial increase in both the α-helical and β-sheet content of CTA1,with a corresponding loss of irregular structure (Fig. 1D, Table 1). Exposure of unfolded CTA1 to Hsp90/ATP did not fully restore the toxin to its native conformation, but CTA1 did gain 11% α-helical content and 18% β-sheet content while losing 26% irregular structure. Hsp90/ATP thus induces a gain-of-structure in the disordered 37°C conformation of CTA1. In contrast, Hsp90/ATPγS did not substantially alter the structure of disordered CTA1 (Fig. 1E, Table 1). ATPγS is a non-hydrolyzable form of ATP. As shown in Figure 1E and Table 1, the gain of structure was dependent on ATP hydrolysis. The chaperone-driven refolding of disordered CTA1 therefore required ATP hydrolysis by Hsp90. Control experiments using FTIR spectroscopy demonstrated that ATP and ATPγS alone had no direct effect on the structure of CTA1 (Fig. 2, Table 2). Additional control experiments using SPR confirmed that Hsp90/ATPγS could, like Hsp90/ATP, bind to CTA1 at physiological temperature (Fig. 3) so the inability of Hsp90/ATPγS to fold CTA1 was not a result of an inability to bind toxin. However, as discussed in the next section, the binding affinity of Hsp90/ATPγS appears to be less than that of Hsp90/ATP.

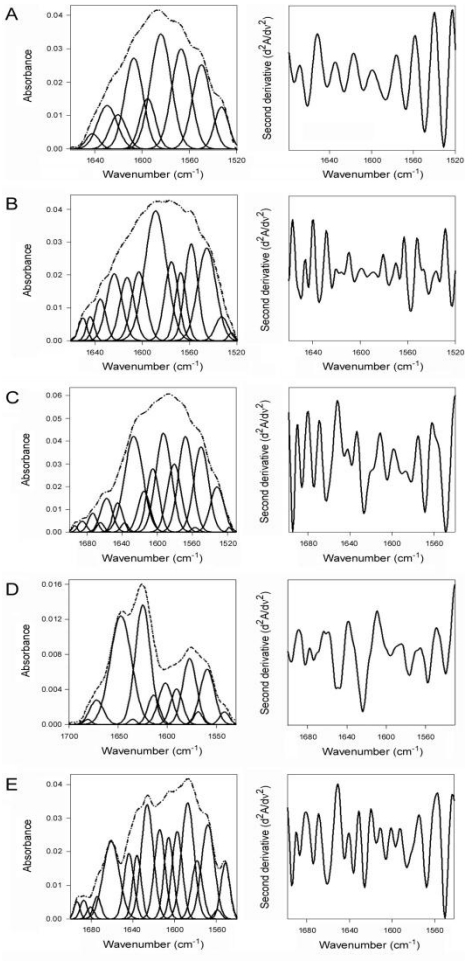

Figure 1. Hsp90/ATP induces a gain-of-structure in disordered CTA1

The FTIR spectrum of ^{13}C-labeled CTA1 was recorded in the absence or presence of Hsp90. In the curve-fitting panels of the left column, the dotted line represents the sum of all deconvoluted components (solid lines) from the measured spectrum (dashed line). The right column presents the respective second derivatives. **A**. CTA1 structure at 10°C. **B**. CTA1 structure at 37°C. **C**. CTA1 structure in the presence of Hsp90 at 37°C. **D**. CTA1 structure in the presence of Hsp90/ATP at 37°C. **E**, CTA1 structure in the presence of Hsp90/ATPγS at 37°C.

Table 1. ATP-driven refolding of CTA1 by Hsp90

	% of CTA1 structure			
Condition	α-Helix	β-Sheet	Irregular	Other
10°C	34 ± 2	42 ± 2	17 ± 2	8 ± 0
37°C	17 ± 1	15 ± 2	54 ± 2	14 ± 1
37°C + Hsp90	20 ± 1	19 ± 3	52 ± 3	9 ± 1
37°C + Hsp90/ATP	28 ± 1	33 ± 2	28 ± 3	11 ± 1
37°C + Hsp90/ATPγS	16 ± 1	12 ± 2	52 ± 2	19 ± 2

Deconvolution of amide I bands from the FTIR spectroscopy data of Figure 1 was used to calculate the percentages of CTA1 structure under the stated conditions. The averages ± standard deviations from three to four individual curve fittings are shown.

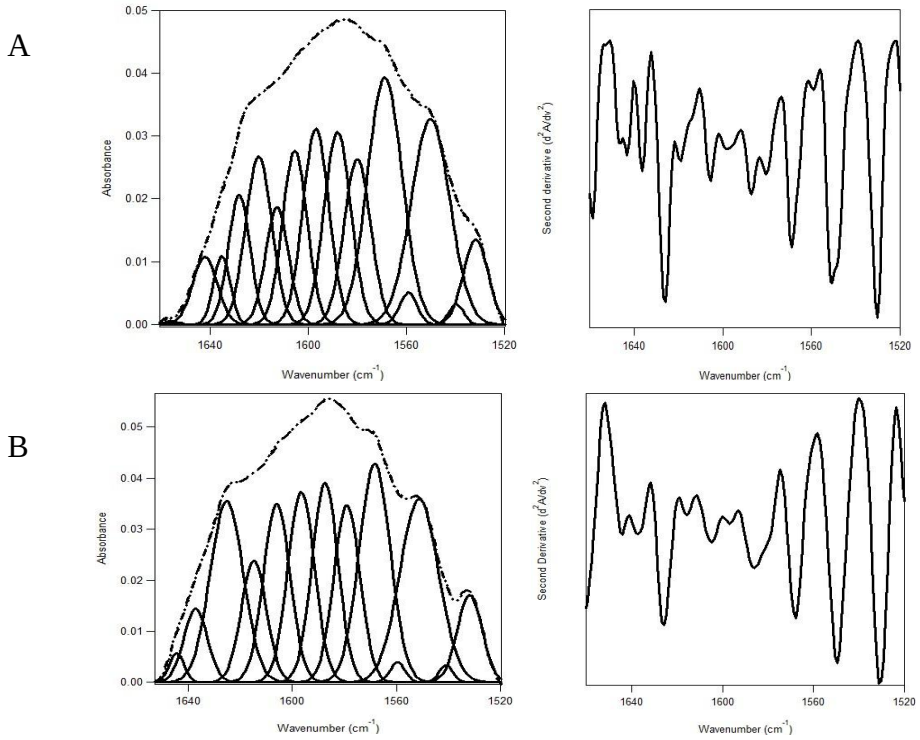

Figure 2. ATP and ATPγS do not affect the structure of CTA1

The FTIR spectrum of ^{13}C-labeled CTA1 was recorded in the presence of ATP and ATPγS. In the curve-fitting panels of the left column, the dotted line represents the sum of all deconvoluted components (solid lines) from the measured spectrum (dashed line). The right column presents the respective second derivatives. **A**. CTA1/ATP structure at 37°C. **B**. CTA1/ATPγS structure at 37°C.

Table 2. Effect of ATP and ATPγS on CTA1 structure

	% of CTA1 structure			
Condition	α-Helix	β-Sheet	Irregular	Other
37°C + ATP	18 ± 2	17 ± 2	54 ± 2	11 ± 1
37°C + ATPγS	25 ± 3	15 ± 1	50 ± 4	10 ± 4

Deconvolution of amide I bands from the FTIR spectroscopy data of Figure 2 was used to calculate the percentages of CTA1 structure under the stated conditions. The averages ± standard deviations from three independent curve fittings is shown.

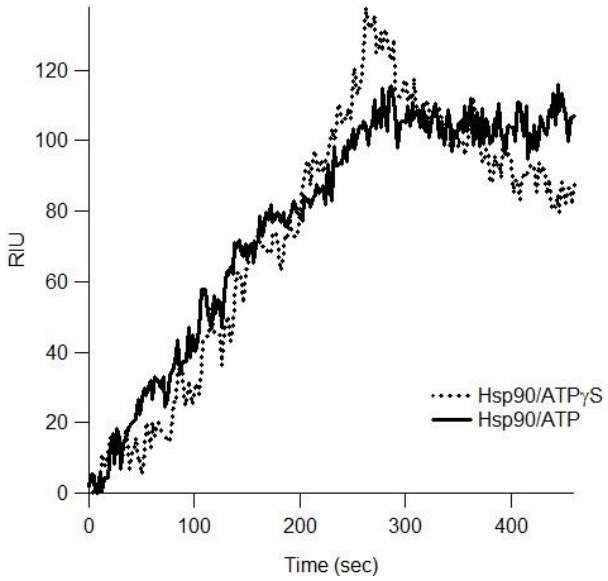

Figure 3. Comparative binding of Hsp90/ATP and Hsp90/ATPγS to CTA1

Hsp90/ATP was perfused over a CTA1-coated sensor slide at 37°C (solid line). Hsp90/ATPγS was perfused over the same sensor slide (dotted line). Ligand was removed from perfusion buffer at approximately 250 sec. Both Hsp90/ATP and Hsp90/ATPγS are able to bind to unfolded CTA1.

ATP hydrolysis by Hsp90 influences its affinity for CTA1

To further investigate the interaction between Hsp90/ATPγS and CTA1 multiple concentrations of Hsp90/ATPγS were perfused over a CTA1-coated SPR sensor at 37°C. A representative experiment is presented in Figure 4, with best fit curves calculated from four independent experiments overlaid on the raw data.

The equilibrium dissociation constant (K_D) between CTA1 and Hsp90/ATPγS was calculated to be 121 μM, which was substantially weaker than the 7 nM previously reported affinity of Hsp90/ATP for CTA1 [37]. Thus, ATP hydrolysis by Hsp90 appears to facilitate the remarkably high affinity interaction between Hsp90 and CTA1.

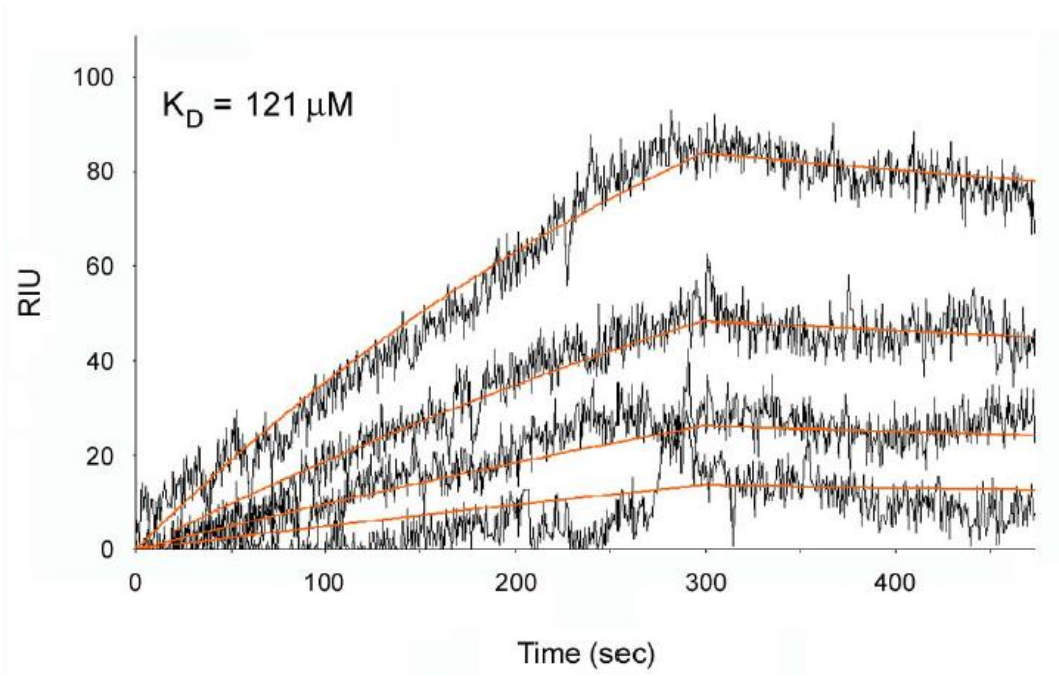

Figure 4. Concentration-dependent binding of Hsp90/ATPγS to CTA1

Five concentrations of Hsp90 (100, 200, 400, 800, 1600 ng/ml) in the presence of 1 mM ATPγS were perfused over a CTA1-coated SPR sensor at 37°C. The 100 ng/ml concentration of Hsp90 is not shown because the signal was not above background levels. Best fit curves (orange lines) derived from four independent experiments were calculated using a 2:1 (Hsp90:CTA1) Langmuir fit. The K_D value of 121 μM was calculated as an average from all four data sets.

ATP hydrolysis by Hsp90 is required for CTA1 extraction from the ER

Cooperative work with Dr. Michael Taylor demonstrated that Hsp90/ATP is sufficient for ER-to-cytosol export of CTA1. CHO cells were exposed to CT for 2 h, permeabilized with digitonin, and separated by centrifugation into cytosolic and intact membrane fractions. The pelleted membranes were washed with 800 mM salt to remove any peripheral membrane associated proteins. The minor pool of Hsp90 which is consistently detected in association with the membrane fraction of digitonin-permeabilized cells [17, 37] was removed by this wash (Fig. 5A). Pelleted membranes were then washed two times with PBS followed by a 5 min centrifugation at 13000 rpm. Wash buffer was removed, and purified Hsp90, ATP, Hsp90/ATP, or Hsp90/ATPγS in HCN buffer was then added to the membrane fraction for 1 h at 4°C. After a 5 min spin at 13000 rpm, the supernatant from the sample was collected and perfused over a SPR sensor coated with an anti-CTA1 antibody. CTA1 translocation across the ER membrane would place it in the supernatant and would accordingly generate a positive SPR signal. Hsp90, Hsp90/ATPγS, and ATP incubated with the membrane fraction did not produce a positive signal as seen in Figure 5B. However, the addition of Hsp90/ATP did provide a positive signal on the anti-CTA1 plate indicating translocation of CTA1 from the ER membrane. Identical results were obtained when the pelleted membranes were washed with 2 M urea instead of 800 mM salt (data not shown). The addition of ATP prior to stripping the membrane also produced a positive signal (data not shown), which is consistent with the previously published work by Winkeler, et al. [50] Using this in vitro reconstitution system to monitor CTA1 export, we discovered that translocation from the ER is dependent upon ATP hydrolysis by Hsp90. The addition of Hsp90, Hsp90/ATPγS, or ATP did not allow the translocation event to occur (Fig. 5B). In view of the

fact that ATP hydrolysis by Hsp90 is also required to refold CTA1, our collective observations support a ratchet model of toxin translocation in which Hsp90 couples CTA1 refolding with extraction from the ER.

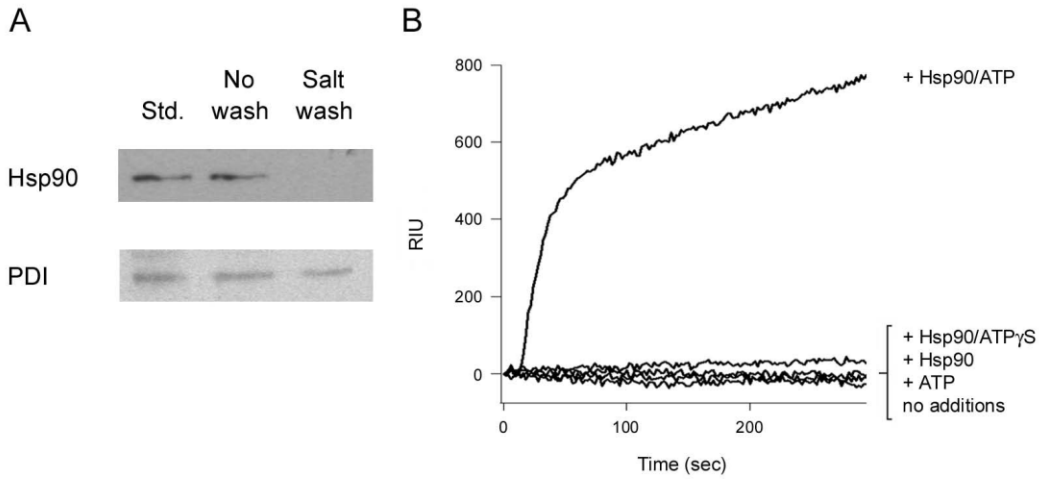

Figure 5. ATP hydrolysis by Hsp90 is required for CTA1 extraction from the ER

CHO cells were intoxicated with CT for 2h prior to digitonin permeabilization in order to ensure a detectable amount of CT was able to reach the ER. The separation of cytosolic components from membrane bound components ensured that no previously translocated CTA1 was detected during the assay. **A**, Western blot verifying the removal of membrane-associated Hsp90 from salt-washed pellets obtained from digitonin-permeabilized cells. **B**, Purified Hsp90, ATP, Hsp90/ATP, or Hsp90/ATPγS in HCN buffer was added to the membrane fraction for 1 h at 4°C. Supernatant samples were obtained after centrifugation, and CTA1 translocation was monitored by SPR. Samples were perfused over and anti-CTA plate to determine the presence of CTA1. CTA1 translocation did not occur with the addition of Hsp90, Hsp90/ATPγS, or ATP. The addition of Hsp90/ATP did provide a positive signal on the anti-CTA plate indicating translocation of CTA1 from the ER membrane.

Hsp90 preferentially binds to disordered CTA1 but is not released after CTA1 refolding

An additional series of SPR experiments was performed to characterize the interaction between Hsp90/ATP and CTA1 (Fig. 6). Hsp90/ATP was perfused over a CTA1-coated sensor slide at 15°C, a temperature that maintains CTA1 in a folded conformation. The minimal interaction between Hsp90 and CTA1 at this temperature (Fig. 6A, dotted line) was not strong enough to calculate a K_D value. The temperature was then increased to 37°C in order to promote the unfolding of CTA1. As expected, Hsp90/ATP bound readily to CTA1 at 37°C (Fig. 6A, solid line). Hsp90 thus appeared to specifically recognize the unfolded conformation of CTA1. In support of this interpretation, we found that Hsp90/ATP could bind to heat-denatured CTA1 at 15°C (Fig. 6B). This demonstrated Hsp90/ATP is functional at low temperature, so the weak interaction between Hsp90/ATP and folded CTA1 at 15°C could be attributed to the conformation of CTA1 rather than to the temperature of the experiment.

Hsp90/ATP interacts specifically with disordered CTA1 (Fig. 6A, B) and will refold the toxin in an ATP-dependent process (Fig. 1, Table1), yet toxin refolding does not appear to result in the dissociation of Hsp90. To further examine this possibility, we perfused Hsp90/ATP over a CTA1 bound sensor slide at 37°C (Fig. 6C). After Hsp90/ATP was removed from the perfusion buffer, the Hsp90-CTA1 complex was cooled to 10°C in a stepwise manner. This process has previously been shown to promote the refolding of disordered CTA1 [14]. The temperature was then increased back to 37°C to allow direct comparison of the RIU signal before and after cooling (temperature has a direct effect on the RIU signal [51, 52]). We recorded identical RIU signals before and after cooling, which indicated Hsp90 did not appreciably dissociate from the temperature-stabilized CTA1 subunit over the time course of the experiment. The continued

presence of Hsp90 on the CTA1-coated sensor slide was verified with an anti-Hsp90 antibody which generated a positive signal when perfused over the sensor slide. Thus, neither the chaperone- or temperature-induced refolding of CTA1 appeared to displace Hsp90 from its binding partner.

Additional SPR experiments were performed to see if specific host factors could promote dissociation of Hsp90 from CTA1. For these experiments, Hsp90/ATP was perfused over a CTA1-coated sensor slide at 37°C. Subsequent perfusions of purified Hsp90 cofactors, the 20S proteasome, 26S proteasome, LUVs mimicking the composition of the plasma membrane or lipid rafts, or the cytosolic fraction from approximately 3.6×10^6 cells failed to separate Hsp90 from CTA1 (Table 3). Although these in vitro studies may not fully replicate the in vivo condition, they suggest Hsp90 does not dissociate from CTA1 after extracting the toxin from the ER.

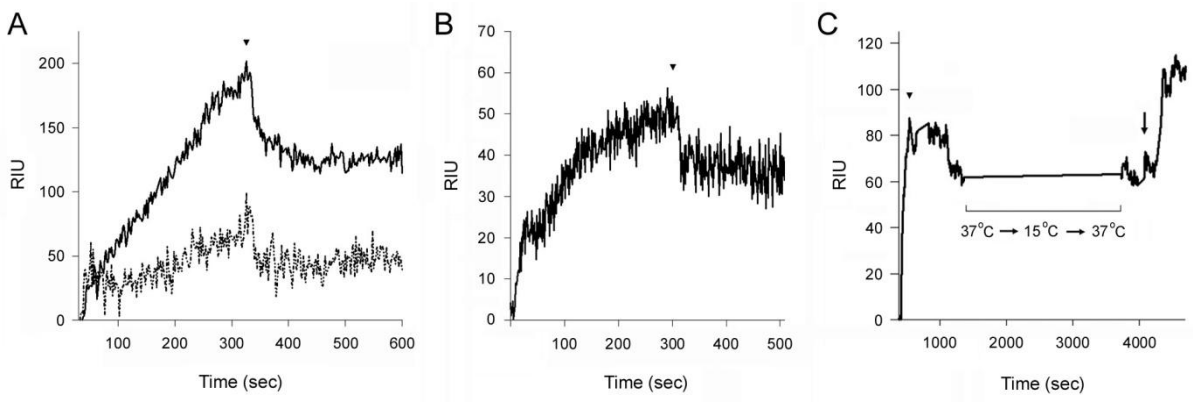

Figure 6. Hsp90 binds unfolded CTA1 and is not released after CTA1 refolding

A, Hsp90/ATP was perfused over a CTA1-coated sensor slide at 15°C (dashed line) or 37°C (solid line). The arrowhead denotes removal of Hsp90/ATP from the perfusion buffer. **B**, Hsp90/ATP was perfused at 15°C over a SPR sensor coated with heat-denatured CTA1. The arrowhead denotes removal of Hsp90/ATP from the perfusion buffer. **C**, Hsp90/ATP was perfused over a CTA1-coated sensor slide at 37°C and was removed from the perfusion buffer after 300 sec (arrowhead). This was followed by a stepwise temperature decrease to 15°C, temperature held for 10 min, followed by increase in temperature back to 37°C. Upon return to 37°C, the continued association of Hsp90 with CTA1 was verified by the addition of an anti-Hsp90 antibody to the perfusion buffer (arrow).

Table 3. Host factors that do not displace Hsp90/ATP from CTA1

CTA1 cofactor	ARF6 Lipid Raft LUVs
Hsp90 cofactor	Hsc70 Hsp40 AHA Hop p23
Other	Cytosolic extract Plasma membrane LUVs 20S proteasome 26S proteasome

Hsp90/ATP was perfused over a CTA1-coated SPR sensor at 37°C. After plateau of the resulting RIU signal, Hsp90 was removed from the perfusion buffer and replaced with one of the listed host factors for a 300 sec perfusion. No decrease in the amount of binding was observed. The continued association of Hsp90 with CTA1 was then confirmed with the addition of an anti-Hsp90 antibody to the perfusion buffer, which provided a positive signal in every case.

Association of CTA1 with Hsp90 does not protect the toxin from proteasomal degradation.

Studies have shown that Hsp90 can play a role in protein degradation dependent upon its association with the proteasome [53, 54]. Coupled with its role as a chaperone, we hypothesized that may protect CTA1 from degradation in the cytosol. To determine if continued association with Hsp90 had an effect on the in vivo turnover of CTA1, we used a plasmid-based system to express CTA1 directly in the host cytosol [21]. Geldanamycin (GA) [55] was then used to inhibit the function of Hsp90 in CTA1-expressing cells. Exogenous application of the CT holotoxin could not be used for this experiment because GA blocks translocation of CTA1 from the ER to the cytosol [37], which would prevent CTA1 from interacting with the proteasome. Plasmid-expressed CTA1 was pulse-labeled with ^{35}S-methionine and chased for up to four hours. The radiolabeled pool of CTA1 immunoprecipitated at 0, 0.5 1, 2, or 4 hours of chase was detected by SDS-PAGE with Biorad Personal Molecular Imager and subsequent Biorad Quantity One analysis (Fig. 7A). The amount of CTA1 remaining in GA-treated cells was not significantly different from the untreated cells (Fig. 7B). In untreated cells, CTA1 exhibited a half-life between 1-2 h as previously reported (Fig. 7B, circles) [56]. These data indicate the association of CTA1 with Hsp90 does not significantly alter proteasomal degradation of CTA1 and does not affect the half-life of the toxin.

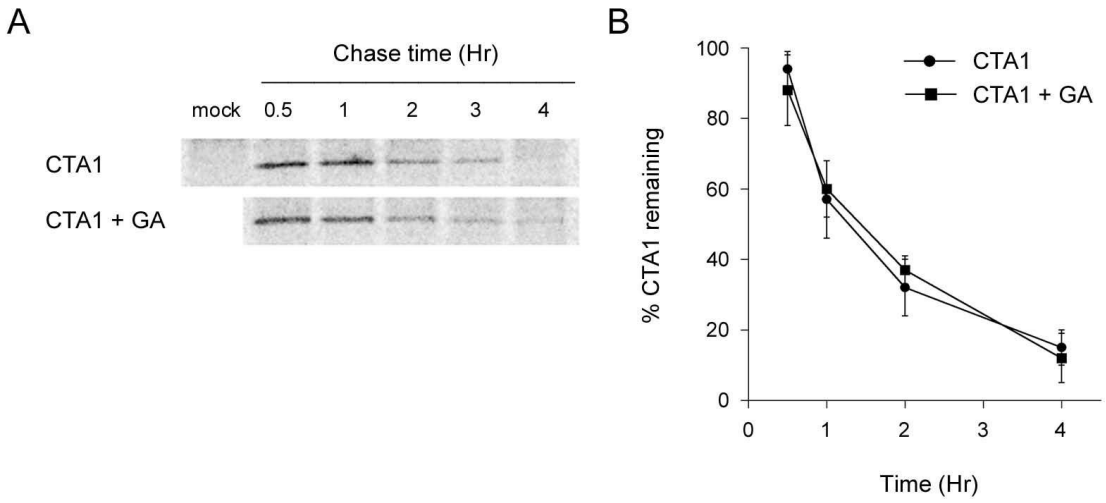

Figure 7. Hsp90 does not protect CTA1 from proteasomal degradation

CTA1 was directly expressed into the cytosol via a plasmid-based expression system that thereby removed the need of Hsp90 for translocation from the ER. Cells were pulse-chased with ^{35}S radiolabeling in the presence or absence of 0.1 μM geldanamycin (GA). Cells were collected, lysed, and subjected to immunoprecipitation with anti-CT bound sepharose beads. **A**, Representative phosphoimage of ^{35}S-labeled CTA1 with and without 0.1 μM GA treatment over four hours. **B,** Graphical representation of degradation minus background lane intensity, with points set as a percentage of the pulse amount of CTA1. The resulting values from 5-6 independent experiments were then averaged, and the standard error of the means is indicated.

Hsp90/ATP enhances the ADP-ribosyltransferase activity of CTA1

To determine the effect of Hsp90 on the activity of CTA1, we performed an in vitro toxicity assay using DEA-BAG as a synthetic substrate for the ADP-ribosyltransferase activity of CTA1 (Fig. 8). The fluorescent output from this assay is directly proportional to the amount of substrate modified by CTA1. As shown in Figure 8A, the folded conformation of CTA1 at 25°C (circles) produced a concentration-dependent increase in the amount of modified DEA-BAG. CTA1 activity at 25°C was slightly elevated in the presence a 2-fold molar amount of Hsp90/ATP (squares), which functions as a dimer. When our ADP-ribosylation assay was repeated at 37°C, the disordered conformation of CTA1 did not produce a concentration-dependent increase in the amount of modified DEA-BAG (Fig. 8B, circles). The baseline signal observed under this condition represents a background reading, as previous work has shown CTA1 and heat-denatured CTA1 produce similar DEA-BAG responses at 37°C. Addition of Hsp90 alone (triangles) or Hsp90/ATPγS (inverted triangles) to the disordered conformation of CTA1 at 37°C had no effect on toxin activity. However, the addition of Hsp90/ATP to disordered CTA1 (Fig 8B, squares) produced a dramatic, concentration-dependent increase in toxin activity. The gain-of-structure in disordered CTA1 resulting from its interaction with Hsp90/ATP thus generated a corresponding gain-of-function for the toxin's ADP-ribosyltransferase activity. This gain-of-function was dependent upon ATP hydrolysis by Hsp90, which was consistent with the structural requirements for CTA1 refolding by Hsp90.

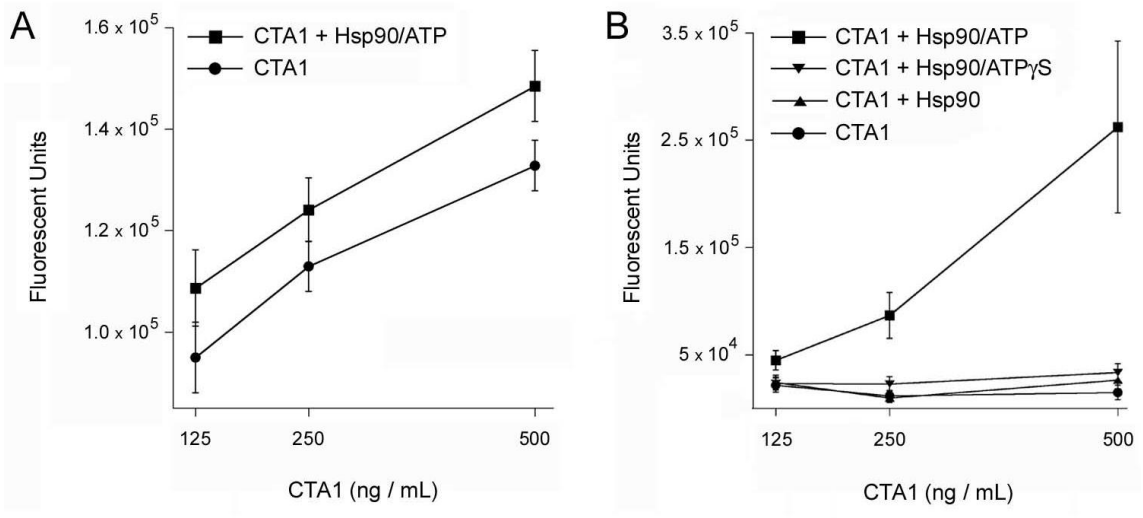

Figure 8. Hsp90/ATP increases the in vitro ADP- ribosylation activity of CTA1

Folded CTA1 was incubated with DEA-BAG, an artificial substrate for ADP-ribosylation, in the presence and absence of Hsp90/ATP. Modification of substrate by CTA1 results in an increased fluorescence signal measured at 440 nm. **A**, The amount of modified substrate in the presence of ordered CTA1 at 25°C (circles) increases in a concentration dependent manner, and the addition of Hsp90/ATP further increases toxin activity (squares). **B**, CTA1 was thermally unfolded by incubation at 37°C for 30 minutes prior to performing the assay. CTA1, CTA1 + Hsp90, and CTA1 + Hsp90/ATPγS at 37°C show no concentration dependent increase in activity. Disordered CTA1 incubated with Hsp90/ATP at 37°C regains activity in a concentration dependent manner (squares). Error bars indicate standard error of the mean of 12-16 replications from 4 independent experiments.

ARF6/GTP can bind and activate the Hsp90-associated CTA1 polypeptide

The GTP-bound form of ARF is an allosteric activator of CTA1 [10, 12], and in vivo CT intoxication requires an interaction between ARF and CTA1 **(**Banerjee, submitted manuscript**)**. To determine if ARF6/GTP could associate with the CTA1-Hsp90 complex, sequential additions of Hsp90/ATP and ARF6/GTP were perfused over a CTA1-bound SPR sensor slide (Fig. 9A). As indicated in the sensorgram, the presence of Hsp90/ATP did not interfere with the binding of ARF6/GTP. Antibodies to both Hsp90 and ARF6 were perfused over the sensor slide to verify their continued association (data not shown). Even though ARF6 was still able to bind in the presence of Hsp90, we had to determine if binding had any effect on the stimulatory activity of ARF6.

We then performed an in vitro toxicity assay to determine if ARF6/GTP could enhance the enzymatic activity of Hsp90-associated CTA1 (Fig. 9B). We found that ARF6 stimulation of CTA1 activity was not inhibited by the presence of Hsp90, rather the addition of both ARF6 and Hsp90 enhanced the activity of CTA1 (Fig. 9B, triangles) in a concentration dependent manner above that of Hsp90 alone (Fig. 9B, squares).

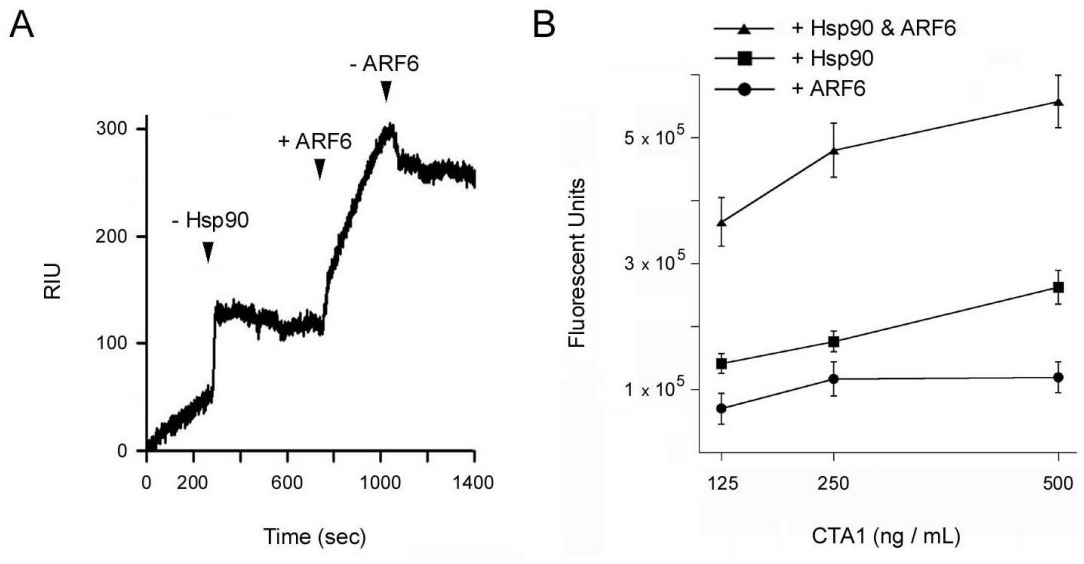

Figure 9. The presence of Hsp90/ATP does not affect the ability of ARF6/GTP to bind and activate CTA1

A, Hsp90/ATP was perfused over a CTA1-coated sensor slide at 37°C and removed from perfusion buffer at 300 sec (first arrowhead). ARF6/GTP was subsequently perfused over the CTA1/Hsp90 complex beginning at 700 sec (second arrowhead) and removed at 1000 sec (third arrowhead). The presence of both Hsp90 and ARF6 on the CTA1 sensor slide were confirmed at the end of the experiment with perfusions of anti-Hsp90 and anti-ARF6 antibodies (data not shown). **B**, ADP-ribosylation assays were performed at 37°C with previously unfolded CTA1 and Hsp90, Hsp90/ARF6, or ARF6. Unfolded CTA1 incubated with both Hsp90 and ARF6 together (triangles) resulted in a higher amount of activity, in a concentration dependent manner, than CTA1 with Hsp90 (squares) or ARF6 (circles) alone. Excess amounts of ATP/GTP were provided in conditions involving Hsp90/ARF6 respectively.

CTA activity is enhanced by host factors in a sequence dependent manner

Lipid rafts on the cytosolic face of the plasma membrane are the site of the G protein target of CTA1 [10-12]. Lipid raft interaction has been shown to induce a gain-of-structure and function in disordered CTA1 [57]. Previous experiments verified that lipid rafts did not dislodge Hsp90 from CTA1 (Table 3). To determine if Hsp90-associated CTA1 could interact with lipid rafts, CTA1 and Hsp90/ATP were incubated at 37°C for ten minutes to allow complex formation and subsequently perfused over a lipid raft LUV-bound sensor slide (Fig. 10A). The bound components were then probed with CTA and Hsp90 antibodies, verifying the presence of both (data not shown).

To assess the relative contributions of host factors to CTA1 activity, various combinations of Hsp90/ATP, ARF6/GTP, and lipid raft LUVs were added to CTA1 in our DEA-BAG activity assay (Fig. 10B-C). Experiments were performed at 37°C to mimic physiological temperature. In Figure 10B, host factors were added to CTA1 after the toxin had been warmed to 37°C for 30 min. Combinations of both ARF6/Hsp90 and ARF6/lipid rafts returned the disordered toxin to a functional state (Fig. 10B). However, toxin activity in the presence of ARF6/Hsp90 was approximately 2-fold greater than the level of activity recorded for the CTA1 sample exposed to a combination of ARF6 and lipid rafts. We hypothesized that a combination of ARF6, Hsp90, and lipid rafts would restore the greatest level of activity to disordered CTA1, but, surprisingly, no activity was observed from the CTA1 sample incubated with all three host factors.

In vivo, CTA1 will interact with Hsp90 before encountering the lipid raft environment where its Gsα target is located. The active, GTP-bound form of ARF6 is associated with membranes as

well [12]. Furthermore, our data indicate Hsp90 remains bound to the cytosolic pool of CTA1 after facilitating the translocation event. We therefore hypothesized that the sequential interactions between CTA1 and Hsp90, followed by contact with ARF6 and lipid rafts, would allow the refolded toxin to maintain an active conformation. To test this model, we warmed CTA1 to 37°C for 30 min and then added either Hsp90, ARF6 and/or lipid rafts. After 1 h at 37°C, the other missing host factor(s) were added for another hour at 37°C. The ADP-ribosylation reaction was then initiated by addition of substrate and NAD and allowed to proceed for 2 h at 37°C. No toxin activity was recorded when all three host factors were added simultaneously, but some level of activity was obtained when lipid rafts were added before ARF6 and Hsp90 (Fig. 10C). A much greater level of activity was recorded when Hsp90 and ARF6 were added before lipid rafts, which suggested the order of host factor interaction is important for CTA1 to achieve maximum activity.

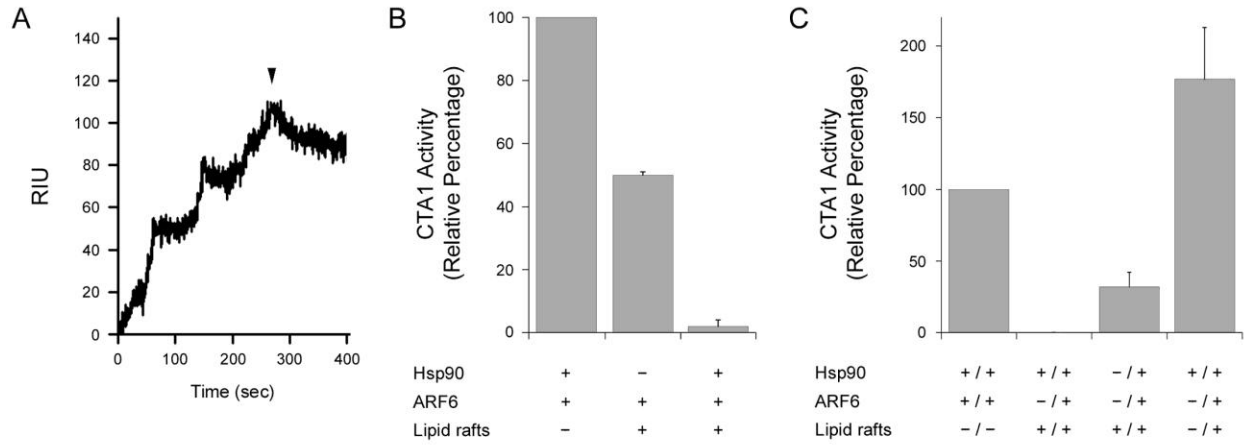

Figure 10. CTA activity is enhanced by host factors in a sequential manner

A, CTA1 and Hsp90/ATP were incubated at 37°C for 10 min at a molar ratio of 1:2 to allow complex formation. The complex was then perfused over a lipid raft LUV coated sensor slide for 300 sec and then removed from the perfusion buffer (arrowhead). The presence of Hsp90 and CTA1 were verified by antibody controls (data not shown). **B**, In vitro ADP-ribosylation activity of CTA1 at 37°C in the presence of indicated host factors. Incubation of disordered CTA1 with Hsp90 and ARF6 lead to the strongest gain of function, while incubation with lipid rafts and ARF6 produced only partial gain of function. The simultaneous addition of lipid rafts with both Hsp90 and ARF6 inhibited CTA1 activity. **C**, Disordered CTA1 was incubated with the first host factor for 1 h at 37°C, followed by the additional host factor(s) for another hour. The activity of CTA1 was then measured. The simultaneous addition of all three host factors inhibited CTA1 activity, while a modest increase in activity was seen with the addition of lipid rafts prior to Hsp90 and ARF6. The addition of Hsp90 and ARF6 prior to the addition of lipid rafts stimulated CTA1 activity above the previously observed maximum activity with Hsp90/ARF6.

Discussion

Cholera toxin binds the cell surface, is internalized and undergoes retrograde transport to the ER where the A1 catalytic subunit dissociates from the holotoxin. Due to the thermal instability of CTA1, it spontaneously unfolds following dissociation. The ERAD system then recognizes unfolded CTA1 and targets the protein to the cytosol for degradation. The translocation of CTA1 from the ER has been shown to be dependent upon the cytosolic chaperone Hsp90. Our structure/function analysis of the interaction of Hsp90 with CTA1 provides molecular details of intoxication that were previously unknown.

Following CTA1 translocation to the cytosol, it must regain its active conformation in order to modify its Gsα target. We have shown by isotope-edited FTIR spectroscopy that Hsp90 refolds CTA1 in an ATP-dependent manner (Fig. 1, Table1). Interestingly, we found that the refolding of CTA1 and high affinity binding of Hsp90 is dependent on hydrolysis of ATP (Fig. 1, 3, 4). Translocation of CTA1 from the ER is also dependent on the ability of Hsp90 to hydrolyze ATP (Fig. 5). These data suggest Hsp90-mediated extraction from the ER is coupled with the refolding event in an ATP-dependent manner.

Further investigation of this interaction has shown that Hsp90/ATP preferentially interacts with unfolded CTA1 (Fig. 6A). This is an example of standard chaperone function, however, once the interaction occurs, Hsp90 remains bound to the folded conformation of CTA1 (Fig. 6C). In order to determine if a host factor was necessary to dislodge Hsp90 from CTA1, we perfused multiple known cytosolic host factors over the bound proteins. Surprisingly, none of the host factors tested would dislodge Hsp90 from CTA1 (Table 3), thus supporting previous data

demonstrating the high affinity interaction [37]. The strength of interaction suggested that Hsp90 remains bound to CTA1 in the cytosol. To determine if this interaction with Hsp90 had any effect on the half life of CTA1, we performed in vivo degradation assays and found that the interaction did not protect CTA1 from proteasomal degradation (Fig. 7). The lack of protection could be due to the fact that CTA1 is still in a partially disordered conformation and is still able to be a substrate for the 20S proteasome.

We then investigated the effect continued association with Hsp90 would have on the activity of CTA1. In vitro ribosylation assays showed that the Hsp90-mediated refolding of CTA1 leads to gain-of-function at physiological temperature (Fig. 8). This increase in activity is dependent on ATP hydrolysis as shown in Figure 8B, consistent with the requirement of hydrolysis for refolding of CTA1 (Fig. 1). Because CTA1 is known to interact with ARF6 [11] and lipid rafts [57], we investigated the effect of continued Hsp90 association on these interactions. Formation of the CTA1/Hsp90 complex did not interfere with binding to these co-factors (Fig. 9A, 10A). Using ADP-ribosylation assays to determine the effect of complex formation on CTA1 activity, we found that the addition of Hsp90/ATP and ARF6 increased the activity of CTA1 above the gain-of-function seen with the addition of Hsp90/ATP alone (Fig. 9B). Interestingly, the addition of Hsp90/ATP, ARF6, and lipid rafts concurrently actually inhibited CTA1 activity (Fig. 10B). We hypothesized that, because CTA1 interacts with host factors in a specific sequence in the cytosol, perhaps the order of interaction was important for activity. We then performed the activity assay by adding the host factors in a sequential manner. The addition of Hsp90/ARF6 to CTA1 before the addition of lipid rafts significantly increased the in vitro activity of CTA1 (Fig. 10C). This data suggest that the initial interaction of CTA1 with Hsp90 is

important for refolding prior to interaction with and lipid rafts. These observations support the model of Hsp90/ATP dependent extraction from the ER, coupled with continued association of Hsp90 in the cytosol until CTA1 reaches host factors that further enhance the activity of CTA1.

Hsp90 was previously shown to be essential for export of CTA1 to the cytosol by both RNAi and drug treatment [37]. These studies also established the requirement of ATP for Hsp90 binding to CTA1. Our work has provided molecular detail to this process that was previously unknown. Surface plasmon resonance studies established that high affinity binding of Hsp90 to CTA1 is dependent on ATP hydrolysis and FTIR analysis determined that refolding of CTA1 is dependent on ATP hydrolysis as well. The requirement of hydrolysis for translocation established by our in vitro reconstitution assay provides further insight into this process. Our results suggest that Hsp90/ATP binds to CTA1 as it emerges from the ER, and the hydrolysis of ATP allows Hsp90 to refold CTA1. This refolding-coupled translocation event acts as a ratchet providing the driving force for extraction of CTA1 from the ER. Association of Hsp90 with CTA1 in the cytosol does not prevent interaction with known CTA1 cofactors and in fact stimulates CTA1 activity in a sequence-dependent manner consistent with the order of interaction expected in the cytosol. Collectively, our data provide evidence that Hsp90 is essential in cholera intoxication both co- and post-translocation. Our data provide new mechanistic details of the modulation of CTA1 structure and function by Hsp90. These findings could also be applied to understanding the ER-to-cytosol export of other p97-independent ADP-ribosylating toxins.

CHAPTER 4 HSP90 AND HSC70 PERFORM OVERLAPPING ROLES IN POST-TRANSLOCATION PROCESSING OF CHOLERA TOXIN

Introduction

Cholera toxin (CT) is an AB_5 toxin that binds the surface of intestinal epithelial cells and travels by vesicle carriers to the endoplasmic reticulum (ER) where the catalytically active A1 subunit is separated from the rest of the toxin [3, 4]. The dissociated CTA1 subunit then spontaneously unfolds due to its intrinsic instability [14] and is processed by the ER-associated degradation (ERAD) system for export to the cytosol [17-19]. CTA1 evades ERAD-mediated degradation in the cytosol [25, 27, 28] and modifies its G protein target to elicit a toxic effect [41-45]. Because CTA1 is an unstable protein, it must be refolded and stabilized by host factors in the cytosol. Our previous studies have shown that Hsp90 actively refolds CTA1. This activity is consistent with its role as a chaperone that refolds endogenous cytosolic proteins as part of a foldosome complex consisting of Hsp90, Hop, p23, Hsp40, and Hsc70 [58-61]. Refolding of unfolded substrates in the cytosol normally occurs via interaction with Hsp40, delivery to Hsc70, and further complex formation with Hop, Hsp90, and p23 [62-64]. Interestingly, Hsp90 and Hsc70 alone have been found to be sufficient for processing of glucocorticoid receptors [65]. Our work has shown that Hsp90 is involved in translocation and refolding of CTA1, however, a role for Hsc70 in CT intoxication has not yet been established. Here, biophysical, biochemical, and cell-based assays demonstrate that Hsp90 and Hsc70 play overlapping roles in the processing of CTA1. Hsc70 binds CTA1 with high affinity in the absence of ATP. The interaction between CTA1 and Hsc70 is essential for intoxication, as an RNAi-induced loss of the Hsc70 protein generates a toxin-resistant phenotype. Studies using isotope-edited FTIR spectroscopy found

that, like Hsp90, Hsc70 induced a gain-of-structure in unfolded CTA1. Binding studies using SPR showed that Hsp90 and Hsc70 could bind independently to CTA1 at distinct locations with high affinity, even in the absence of the Hop linker. Further FTIR analysis demonstrated that the addition of Hsc70 and Hsp90 to unfolded CTA1 induced a gain-of-structure above that of Hsp90 or Hsc70 alone. Collectively, these results suggest that their cooperative refolding would increase the catalytic activity of CTA1 above the level of independent association and that Hsc70 plays a vital role in the processing of CTA1.

Hsc70 binds unfolded CTA1 in the absence of ATP with high affinity

In order to determine if Hsc70 was able to bind to CTA1, we performed SPR analysis. Due to the fact that previous work has found that Hsc70 binding is dependent upon the presence of ATP [62, 66], we perfused the same concentration of Hsc70 with and without ATP over the CTA1 coated sensor slide at 37°C. We found that Hsc70 was able to bind to CTA1 in the absence but not in the presence of ATP (Figure 11A). Previous studies have found that Hsc70 is able to bind other substrates in this manner as well [67, 68]. Because of the relative high affinity for CTA1 observed during the binding assay, we performed further analysis by SPR. We perfused multiple concentrations of Hsc70 over a CTA1-coated sensor slide at 37°C. The resulting concentration-dependent binding is represented in Figure 11B, with the best fit curves from 5 independent experiments overlaid on the raw data. The equilibrium dissociation constant (K_D) between CTA1 and Hsc70 was calculated to be 4.5 nM, which indicates a very high affinity between the two proteins.

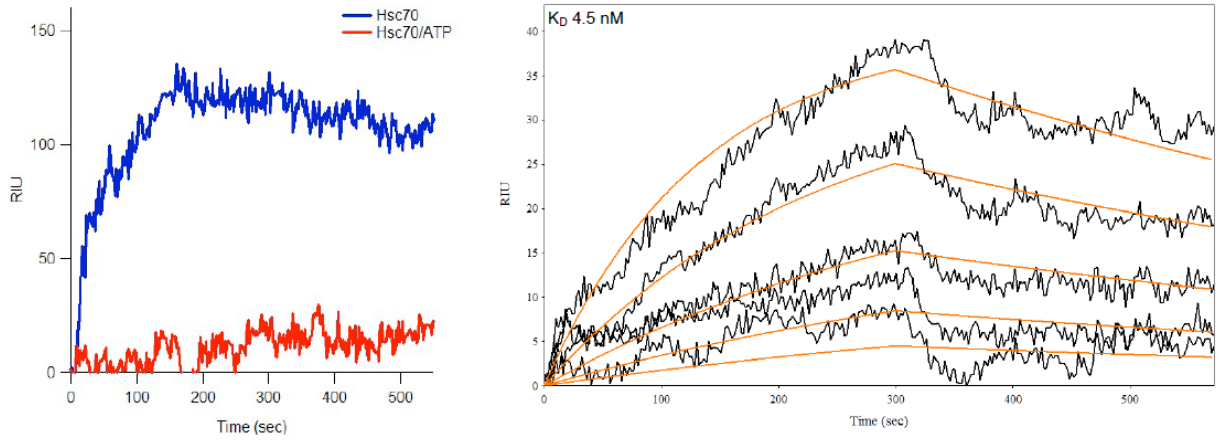

Figure 11. Hsc70 binds unfolded CTA1 in the absence of ATP with high affinity

A, Identical concentrations of Hsc70 (blue line) and Hsc70/ATP (red line) were perfused over a CTA1-coated SPR sensor at 37°C. Hsc70 ± ATP was removed from the perfusion buffer at 200 seconds. The absence or presence of Hsc70 was verified by anti-Hsc70 antibody (data not shown). **B**, Five concentrations of Hsc70 (100, 200, 400, 800, 1600 ng/ml) were perfused over a CTA1-coated SPR sensor at 37°C. Hsc70 was removed from the perfusion buffer at 300 sec. Best fit curves (orange lines) derived from five independent experiments were calculated using a 1:1 (Hsc70:CTA1) Langmuir fit. The presented K_D value was calculated from all five data sets.

Hsc70 induces a gain-of-structure in disordered CTA1

Preliminary data has shown that the interaction of CTA1 with Hsc70 has an effect on CTA1 activity. Partial knockdown of Hsc70 by siRNA led to complete inhibition of CTA1 activity (A. Romero and K. Teter, unpublished observations). We then investigated what effect binding of Hsc70 had on the structure of CTA1. Hsc70 has been shown to allow refolding of disordered client proteins [65, 69, 70]. Determination of the effect of Hsc70 on the folding state of disordered CTA1 was performed by isotope-edited FTIR spectroscopy (Fig.12). Uniformly ^{13}C-labeled CTA1 was used in order to differentiate between the spectra of CTA1 and unlabeled Hsc70 as previously described. The spectra of CTA1 alone (Fig. 12A) showed that, at 10°C, CTA1 is in a folded conformation with approximately 36% α-helical, 39% β-sheet, and 17% irregular structure (Table 4) consistent with previous work (Fig. 1, Table 1). Increasing the temperature to 37°C caused CTA1 to unfold and lose the majority of its α-helical and β-sheet components while increasing the amount of irregular structure to 54% (Fig. 12B, Table 4). The addition of Hsc70 to previously unfolded CTA1 allowed CTA1 to regain a substantial amount of α-helical and β-sheet content (Fig. 12C, Table 4). CTA1 regained 15% α-helical content, 10% β-sheet content and lost 25% of irregular structure. The addition of ATP to Hsc70 prior to incubation with unfolded CTA1 dramatically reduced the refolding achieved by the addition of Hsc70 alone (Fig. 12D, Table 4). This evidence is consistent with the inability of Hsc70 to bind to CTA1 in the presence of ATP (Fig. 11A).

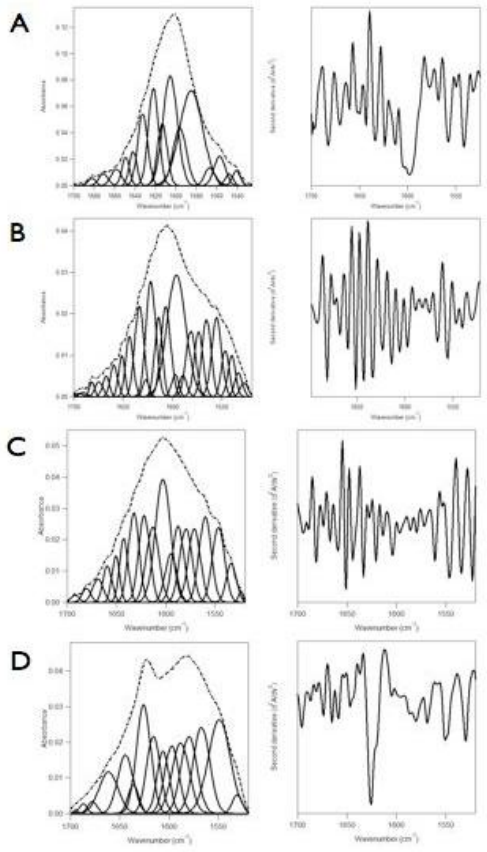

Figure 12. Hsc70 induces a gain-of-structure in disordered CTA1

The FTIR spectrum of ^{13}C-labeled CTA1 was recorded in the absence or presence of Hsc70. In the curve-fitting panels of the left column, the dotted line represents the sum of all deconvoluted components (solid lines) from the measured spectrum (dashed line). The right column presents the respective second derivatives. CTA1 samples incubated with Hsc70 were first heated to 37°C for 30 min prior to addition of equimolar Hsc70. **A**, CTA1 structure at 10°C. **B**, CTA1 structure at 37°C. **C**, CTA1 structure in the presence of Hsc70 at 37°C. **D**, CTA1 structure in the presence of Hsc70/ATP at 37°C.

Table 4. Gain-of-structure induced in disordered CTA1 by Hsc70

Condition	% of CTA1 structure			
	α-Helix	β-Sheet	Irregular	Other
10°C	36 ± 1	39 ± 1	17 ± 2	9 ± 1
37°C	18 ± 2	16 ± 2	54 ± 3	12 ± 2
37°C + Hsc70	33 ± 1	26 ± 2	29 ± 3	13 ± 2
37°C + Hsc70 + ATP	25 ± 2	20 ± 2	43 ± 3	12 ± 2

Deconvolution of amide I bands from the FTIR spectroscopy data of Figure 12 was used to calculate the percentages of CTA1 structure under the stated conditions. The averages ± standard deviations from three to four individual curve fittings are shown.

Hsc70 and Hsp90 can bind CTA1 independently or in a complex with Hop

Hsc70 and Hsp90 have been reported to bind distinct sites on their client proteins [60, 65, 71]. In order to investigate the binding interactions of Hsc70 and Hsp90 with CTA1, we performed a series of SPR experiments. We perfused Hsp90/ATP over a CTA1-coated sensor slide at 37°C for 300 sec and then removed Hsp90/ATP from the perfusion buffer. After allowing the stabilization of the refractive index units (RIU) corresponding to the mass of Hsp90/ATP bound to CTA1, we then perfused Hsc70 over the sensor slide (Fig. 13A). Both Hsp90 and Hsc70 were able to bind to the unfolded CTA1 in the absence of Hop. This is consistent with other reports that Hsp90 and Hsc70 are able to bind endogenous substrates in the absence of Hop [65, 72]. We then investigated whether the addition of Hop had an effect on the binding of Hsc70 to the complex, as this is the normal route of complex formation [63, 73]. The experiment was repeated with the addition of Hop following the binding of Hsp90/ATP on the CTA1-coated sensor slide (Fig. 13B). Hsc70 was then perfused over the sensor slide and binding indicated by the increase in RIU. Antibodies were perfused over the sensor slides to verify the bound components following the experiments (data not shown). The data indicate that Hsc70 and Hsp90 can bind in the presence or absence of the Hop linker. A previous study indicated that Hsp90 and Hsc70 interact weakly with each other [74]. To ensure that the increased RIU signal was not due to an interaction of Hsp90 with Hsc70, we performed additional SPR experiments. Hsc70 was appended to a sensor slide via amide linkage and CTA1 was perfused over the sensor slide at 37°C followed by perfusion of Hsp90/ATP (Fig. 14A). CTA1 was able to bind to the Hsc70-coated sensor slide, and the following perfusion of Hsp90/ATP bound to CTA1. The presence of bound proteins was verified by anti-CTA and anti-Hsp90 antibody perfusions at the

end of the experiment (data not shown). These experiments also verified that Hsc70 was binding a distinct site on CTA1. The increase in RIU in Figure 13A could have been due to Hsc70 binding to unbound CTA1 at the same site as Hsp90. The use of an Hsc70-bound sensor slide ensured that all CTA1 binding sites on Hsc70 would be occupied by CTA1 prior to addition of Hsp90. The interaction of Hsp90 directly with Hsc70 was examined in Figure 14B. Hsp90/ATP was perfused over an Hsc70-coated sensor slide and the resulting RIU recorded. Only minimal, weak interaction was observed in the absence of CTA1. These data indicate that Hsp90 and Hsc70 bind distinct sites on CTA1 and can bind in the presence or absence of Hop.

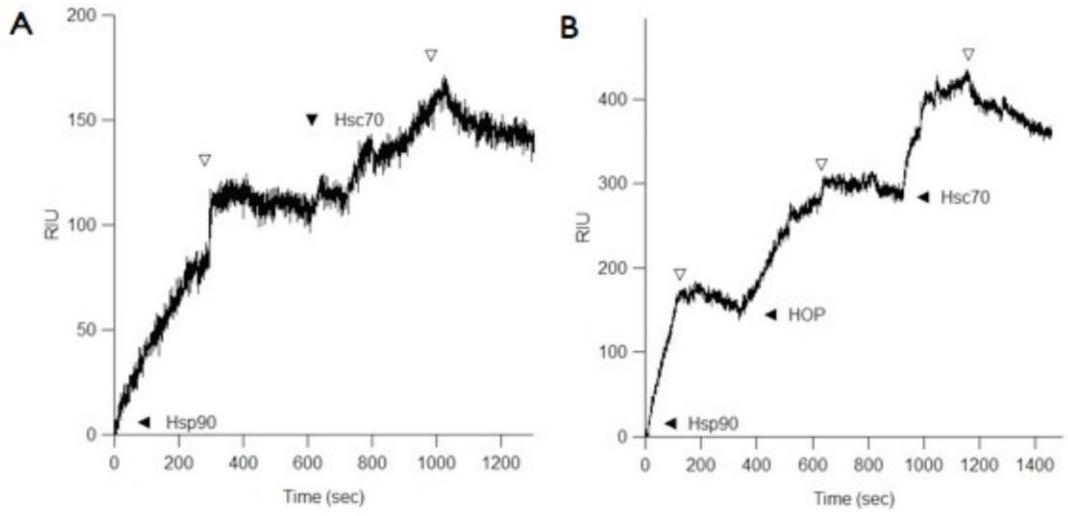

Figure 13. Hsc70 and Hsp90 can bind CTA1 independently or in a complex with Hop

A, Hsp90/ATP was perfused over a CTA1-coated SPR slide at 37°C. After removing Hsp90 from the perfusion buffer (first empty triangle), Hsc70 was then perfused over the sensor slide (solid triangle). Removal of Hsc70 from the perfusion buffer is indicated by the second empty triangle. **B**, Hsp90/ATP was perfused over a CTA1-coated sensor slide at 37°C (solid triangle) and removed from the perfusion buffer (first empty triangle). Hop was then perfused over the CTA1/Hsp90 complex (second solid arrow) and removed from perfusion buffer (second empty triangle). Hsc70 was then perfused over the CTA1/Hsp90/Hop complex (third solid triangle) and removed from perfusion at the third empty triangle. Antibodies confirmed the presence of bound proteins on the sensor slide at the conclusion of each experiment (data not shown).

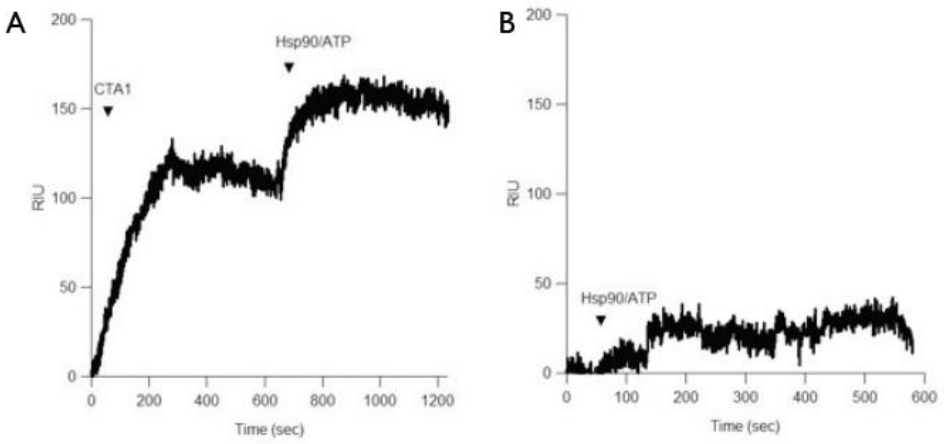

Figure 14. CTA1 binding to Hsc70 prior to addition of Hsp90

A, CTA1 was perfused over an Hsc70-coated sensor slide at 37°C (first arrow). CTA1 was removed from buffer at 300 sec, followed by perfusion of Hsp90 pre-bound with ATP and removal at 1000 sec. **B**, Hsp90 pre-bound with ATP was perfused over an Hsc70-coated sensor slide at 37°C in the absence of CTA1. Antibodies confirmed the presence or absence of bound proteins on the sensor slide at the conclusion of each experiment (data not shown).

Combined impact of Hsc70 and Hsp90 on CTA1 structure

The ability of both Hsc70 and Hsp90 to bind CTA1 at distinct sites suggested a possible cooperative effect on the refolding of CTA1. We then performed isotope-edited FTIR spectroscopy to examine the effect of both proteins on the folding state of CTA1 using uniformly ^{13}C-labeled CTA1 to differentiate between the spectra of CTA1 and unlabeled Hsc70 and Hsp90. ^{13}C-labeled CTA1 was warmed to 37°C for 30 min prior to addition of 2-fold molar excess Hsp90 pre-bound to ATP and equimolar Hsc70. Following a 10 min incubation, the spectra was recorded. Analysis of the spectra showed that the addition of Hsc70 and Hsp90 allowed CTA1 to regain both α-helical and β-sheet content to approximately that of folded CTA1 (Fig. 15 A,B, Fig. 12, Table 4).

A

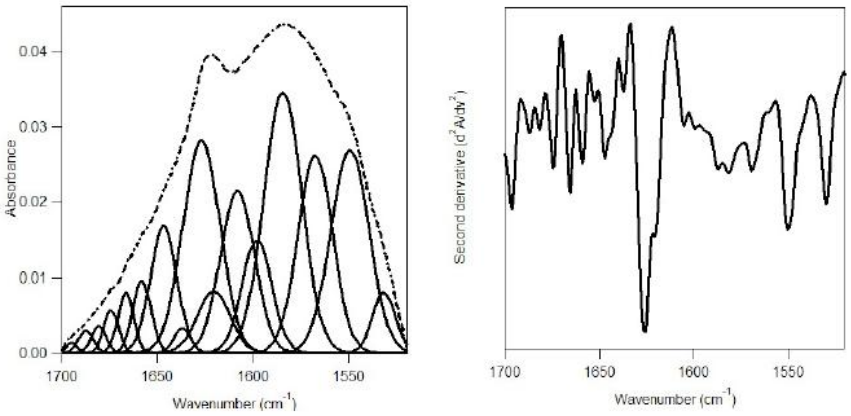

B

Condition	% of CTA1 structure			
	α-Helix	β-Sheet	Irregular	Other
37°C + Hsc70 + Hsp90/ATP	30 ± 2	45 ± 3	18 ± 2	7 ± 1

Figure 15. Combined impact of Hsc70 and Hsp90 on CTA1 structure

A, ^{13}C-labeled CTA1 was heated to 37°C for 30 min before addition of equimolar Hsc70 and 2-fold molar excess of Hsp90 pre-bound to ATP for an additional 10 min at 37°C. Curve fitting (left panel) and second derivative (right panel) for the FTIR spectrum shown. For curve fitting, the dotted line represents the sum of all deconvoluted components (solid lines) from the measured spectrum (dashed line). **B**, Deconvolution of amide I bands from the FTIR spectroscopy data of panel A was used to calculate the percentages of CTA1 structure in the presence of Hsc70 and Hsp90/ATP. The averages ± standard deviations from four independent curve fittings are shown.

Discussion

Cholera toxin is AB_5 toxin that binds the surface of intestinal epithelial cells and travels by vesicle carriers to the ER where the catalytically active A1 subunit is processed by the ERAD system for export to the cytosol. Because CTA1 is an unstable protein, it must be refolded and stabilized by host factors in the cytosol. Our studies have shown that Hsp90 is involved in translocation and refolding of CTA1 (Chapter 3). We have demonstrated by biophysical, biochemical, and cell-based assays that Hsp90 and Hsc70 play overlapping roles in the processing of CTA1.

Our preliminary studies showed that the interaction between CTA1 and Hsc70 is essential for intoxication. Partial loss of the Hsc70 protein through RNAi generates a toxin-resistant phenotype (unpublished observation). While Hsc70 normally interacts with unfolded substrates in the presence of ATP [62, 66], we found that Hsc70 is able to bind to CTA1 in the absence of ATP and binding is inhibited by the presence of ATP (Fig. 11A). Other studies have also shown that the ATP-dependent binding is substrate specific [67, 68]. Due to apparent high affinity binding observed during this binding assay, we perfused multiple concentration of Hsc70 over a CTA1-coated sensor slide to determine the equilibrium dissociation constant (K_D). We found that Hsc70 has a high affinity for CTA1, $K_D \approx 4.5$ nM (Fig. 11B).

Analysis of the effect of Hsc70 binding on the structure of CTA1 was performed using isotope-edited FTIR spectroscopy. We found that the addition of Hsc70 to unfolded CTA1 at 37°C induces a gain-of-structure in unfolded CTA1 (Fig.12C, Table 4). This regain-of-structure was inhibited when ATP was incubated with Hsc70 prior to its addition to CTA1 (Fig. 12D, Table 4).

The lack of folding observed is consistent with the inability of Hsc70/ATP to bind to CTA1 (Fig. 11A).

Our previous work has shown that CTA1 translocation from the ER and refolding is dependent upon Hsp90 (Chapter 3). However, typical foldosome activity begins with substrate binding to Hsp40, delivery to Hsc70 and further complex formation with Hop and Hsp90 [58-61]. Binding assays were performed to determine if Hsc70 was able to bind to CTA1 in the presence of Hsp90. We found that Hsp90 and Hsc70 bind distinct sites on CTA1 and are able to bind independently of other foldosome components (Fig. 13, 14). These results, taken together with the gain-of-structure studies, indicated that a possible cooperative refolding event may be occurring. Further isotope-edited FTIR studies were performed with unfolded CTA1 and both Hsc70 and Hsp90. Analysis of the results confirmed that, in the presence of both chaperones, CTA1 achieved a higher regain of structure than with either chaperone alone (Fig. 15).

Our results suggest that Hsc70 binds CTA1 after its interaction with Hsp90. The binding of both chaperones allows CTA1 to achieve a higher degree of folding. We have shown that this binding occurs in the absence of other foldosome components and in a sequence not typical of unfolded substrates. Our data provide insight into a non-canonical sequence of refolding that has not been previously observed and a role of Hsc70 in the CT intoxication process that was previously unknown.

CHAPTER 5 GENERAL DISCUSSION

The catalytic subunit of cholera toxin (CTA1) is a thermally unstable protein and is largely misfolded at physiological temperature. Despite this intrinsic thermal instability, CTA1 is able to translocate from the ER to the cytosol and elicit its toxic effect through the ADP-ribosylation of the Gsα subunit of the heterotrimeric G protein. In order for CTA1 to gain activity in the cytosol, it must escape the ER into the cytosol and be refolded. While many steps of intoxication are well known, very little is known about the factors involved in translocation and post-translocation processing of CTA1.

Prior work by Taylor et al [37] found that translocation was dependent upon the cytosolic chaperone Hsp90; however, the details of this mechanism were still unknown. Through our biophysical, biochemical, and cell-based assays, we have elucidated many of these details. Our work has shown that Hsp90 causes a gain-of-structure in CTA1 in an ATP-dependent manner. While this is consistent with typical Hsp90 chaperone activity, we also observed, by using a non-hydrolyzable form of ATP (ATPγS), that the hydrolysis of ATP substantially increases the affinity of Hsp90 for CTA1. We then investigated of the effect of ATP hydrolysis on translocation of CTA1 from the ER to the cytosol. Our in vitro translocation assay found that the translocation event is dependent upon the ability of Hsp90 to hydrolyze ATP. These data support our hypothesis that CTA1 translocation is coupled to the refolding of CTA1 by Hsp90 and that the refolding event itself provides the driving force for translocation.

Interestingly, further analysis of the interaction between Hsp90 and CTA1 using SPR revealed that even after the refolding event occurs, CTA1 remains bound to Hsp90. This type of

continued interaction is not consistent with typical chaperone behavior, but we believe that because of the thermal instability of CTA1 and the high affinity binding with Hsp90, CTA1 is not released as other endogenous substrates. Hsp90 has been known to associate with the proteasome during endogenous refolding/degradation events, so we used metabolic labeling to determine if Hsp90 was influencing the half-life of CTA1 in the cytosol. Inhibition of Hsp90 did not affect the half life of cytosolic CTA1, indicating that Hsp90 is neither delivering CTA1 to the proteasome nor protecting it from degradation.

We then investigated the effect of Hsp90 binding on CTA1 activity. Using in vitro ADP-ribosylation assays, we determined that CTA1 activity is significantly increased by Hsp90/ATP binding, but is not affected by Hsp90/ATPγS. This observation is consistent with the ability of Hsp90 to refold CTA1 in the presence of ATP, but not ATPγS. Further studies showed that the continued association with Hsp90 did not interfere with the ability to bind to a known co-factor of CTA1, ARF6. We found through SPR analysis that both proteins could in fact bind CTA1 at the same time. We investigated the ADP-ribosylation activity of CTA1 in the presence of both Hsp90 and ARF6 and found that activity was significantly increased above that of Hsp90 alone.

Recent studies by Ray et al [57] showed that the lipid raft environment that CTA1 encounters during ADP-ribosylation of Gsα acts as a lipochaperone and allows CTA1 refolding to occur. We performed binding assays and found that the binding of Hsp90 and CTA1 did not interfere with interaction of the complex with lipid rafts. The subsequent activity assays performed found that, while the addition of lipid rafts/ARF6 or Hsp90/ARF6 increased ribosylation activity, the simultaneous addition of all three host factors inhibited activity. Further investigation found that

the sequence of host factor binding is critical for CTA1 activity. These data indicate that CTA1 must initially interact with Hsp90, followed by interaction with ARF6 and lipid rafts to achieve maximal activity. This sequence-dependent interaction mimics the order in which host factors would be encountered by CTA1 in the cellular environment.

We then considered other cytosolic factors that may be involved in the processing of CTA1. Hsp90 normally interacts with other members of the foldosome complex, consisting of Hsc70, Hsp40, p23, and Hop. From preliminary evidence obtained by A. Romero (unpublished observations), we knew that knockdown of Hsc70 by siRNA inhibited the activity of CTA1. We then investigated the interaction of Hsc70 with CTA1 directly. We found, through binding assays, that CTA1 binds to Hsc70 in the absence of but not presence of ATP. While most Hsc70 substrate binding is dependent upon the presence of ATP, studies have noted that the requirement of ATP can be substrate-dependent. Our further studies showed that this was a high affinity interaction similar to that observed with Hsp90.

In order to investigate the effect of Hsc70 binding on the structure of CTA1, we performed FTIR analysis that demonstrated the Hsc70 interaction allowed CTA1 to regain partial structure. The regain in structure did not occur in the presence of ATP, consistent with the results from the binding assay.

Normally, unfolded proteins are first bound by Hsp40, delivered to Hsc70, followed by association of Hop, Hsp90 and p23. However, due to the previous data collected on Hsp90 interaction with CTA1 and the preliminary data showing inhibition of activity with Hsc70 knockdown, we investigated the possibility that this was not typical foldosome activity. We then

performed a series of binding assays and determined that Hsc70 and Hsp90 bound to CTA1 at distinct locations. We also discovered that Hsc70 and Hsp90 could bind in the presence or absence of Hop, which normally serves as a linker between Hsp90 and Hsc70.

Due to the ability of both Hsp90 and Hsc70 to bind CTA1, we then performed FTIR analysis to determine their combined effect on CTA1 structure. We determined that, in the presence of Hsp90 and Hsc70, CTA1 regains more structure than when incubated with either chaperone alone. This observation suggests that while Hsp90 extracts CTA1 from the ER and begins the refolding process, Hsc70 binding is required for optimal gain-of-structure. Collectively, our results provide details on mechanisms of cholera intoxication that were not previously known. The data collected may be applicable to other AB_5 toxins that rely on export from the ER as well. We have identified host proteins that interact with a non-native substrate in a manner not previously described and our work provides new insight into the flexibility of host chaperone activity.

REFERENCES

1. Zhang, R.G., et al., *The three-dimensional crystal structure of cholera toxin.* Journal of Molecular Biology, 1995. **251**(7658473): p. 563-73.

2. De Haan, L. and T.R. Hirst, *Cholera toxin: a paradigm for multi-functional engagement of cellular mechanisms (Review).* Molecular Membrane Biology, 2004. **21**(15204437): p. 77-92.

3. Wernick, N.L., et al., *Cholera Toxin: An Intracellular Journey into the Cytosol by Way of the Endoplasmic Reticulum.* Toxins, 2010: p. 1-16.

4. Lencer, W.I., et al., *Mechanism of cholera toxin action on a polarized human intestinal epithelial cell line: role of vesicular traffic.* The Journal of Cell Biology, 1992. **117**(1318883): p. 1197-1209.

5. Orlandi, P.A., *Protein-disulfide isomerase-mediated reduction of the A subunit of cholera toxin in a human intestinal cell line.* The Journal of Biological Chemistry, 1997. **272**(9020187): p. 4591-9.

6. Majoul, I., D. Ferrari, and H.D. Soling, *Reduction of protein disulfide bonds in an oxidizing environment. The disulfide bridge of cholera toxin A-subunit is reduced in the endoplasmic reticulum.* FEBS letters, 1997. **401**(9013867): p. 104-8.

7. Tsai, B., et al., *Protein disulfide isomerase acts as a redox-dependent chaperone to unfold cholera toxin.* Cell, 2001. **104**(11290330): p. 937-48.

8. Taylor, M., et al., *Protein-disulfide Isomerase Displaces the Cholera Toxin A1 Subunit from the Holotoxin without Unfolding the A1 Subunit.* Journal of Biological Chemistry, 2011. **286**(25): p. 22090-22100.

9. Taylor, M., et al., *Substrate-induced unfolding of protein disulfide isomerase displaces the cholera toxin A1 subunit from its holotoxin.* PLoS Pathog, 2014. **10**(2): p. e1003925.

10. O'Neal, C.J., et al., *Structural basis for the activation of cholera toxin by human ARF6-GTP.* Science (New York, NY), 2005. **309**(16099990): p. 1093-6.

11. Welsh, C.F., J. Moss, and M. Vaughan, *ADP-ribosylation factors: a family of approximately 20-kDa guanine nucleotide-binding proteins that activate cholera toxin.* Molecular and Cellular Biochemistry, 1994. **138**(1-2): p. 157-66.

12. Kahn, R.A. and A.G. Gilman, *Purification of a protein cofactor required for ADP-ribosylation of the stimulatory regulatory component of adenylate cyclase by cholera toxin.* J Biol Chem, 1984. **259**(10): p. 6228-34.

13. Harris, J.B., et al., *Cholera.* Lancet, 2012. **379**(9835): p. 2466-76.

14. Pande, A.H., et al., *Conformational instability of the cholera toxin A1 polypeptide.* Journal of Molecular Biology, 2007. **374**(17976649): p. 1114-28.

15. Teter, K., *Toxin Instability and Its Role in Toxin Translocation from the Endoplasmic Reticulum to the Cytosol.* Biomolecules, 2013. **3**: p. 997-1029.

16. Teter, K., *Cholera Toxin Interactions with Host Cell Stress Proteins*. Moonlighting Cell Stress Proteins in Microbial Infections, ed. B. Henderson. Vol. Heat Shock Proteins 7. 2013: Springer Science.

17. Massey, S., et al., *Stabilization of the Tertiary Structure of the Cholera Toxin A1 Subunit Inhibits Toxin Dislocation and Cellular Intoxication.* Journal of Molecular Biology, 2010. **393**(5): p. 1083-1096.

18. Teter, K. and R.K. Holmes, *Inhibition of endoplasmic reticulum-associated degradation in CHO cells resistant to cholera toxin, Pseudomonas aeruginosa exotoxin A, and ricin.* Infect Immun, 2002. **70**(11): p. 6172-9.

19. Teter, K., et al., *Transfer of the cholera toxin A1 polypeptide from the endoplasmic reticulum to the cytosol is a rapid process facilitated by the endoplasmic reticulum-associated degradation pathway.* Infection and Immunity, 2002. **70**(12379694): p. 6166-71.

20. Taylor, M., et al., *A therapeutic chemical chaperone inhibits cholera intoxication and unfolding/translocation of the cholera toxin A1 subunit.* PloS one, 2011. **6**(4): p. e18825.

21. Teter, K., M.G. Jobling, and R.K. Holmes, *A class of mutant CHO cells resistant to cholera toxin rapidly degrades the catalytic polypeptide of cholera toxin and exhibits increased endoplasmic reticulum-associated degradation.* Traffic, 2003. **4**(4): p. 232-42.

22. Banerjee, T., et al., *Contribution of subdomain structure to the thermal stability of the cholera toxin A1 subunit.* Biochemistry, 2010. **49**(20839789): p. 8839-46.

23. Nakatsukasa, K. and J.L. Brodsky, *The recognition and retrotranslocation of misfolded proteins from the endoplasmic reticulum.* Traffic, 2008. **9**(6): p. 861-70.

24. Bagola, K., et al., *Protein dislocation from the ER.* Biochim Biophys Acta, 2011. **1808**(3): p. 925-36.

25. Hazes, B. and R.J. Read, *Accumulating evidence suggests that several AB-toxins subvert the endoplasmic reticulum-associated protein degradation pathway to enter target cells.* Biochemistry, 1997. **36**(9333321): p. 11051-4.

26. Spooner, R.A. and J.M. Lord, *How ricin and Shiga toxin reach the cytosol of target cells: retrotranslocation from the endoplasmic reticulum.* Curr Top Microbiol Immunol, 2012. **357**: p. 19-40.

27. Rodighiero, C., et al., *Role of ubiquitination in retro-translocation of cholera toxin and escape of cytosolic degradation.* EMBO reports, 2002. **3**(12446567): p. 1222-7.

28. Marshall, R.S., et al., *The role of CDC48 in the retro-translocation of non-ubiquitinated toxin substrates in plant cells.* The Journal of Biological Chemistry, 2008. **283**(18420588): p. 15869-77.

29. Orlowski, M. and S. Wilk, *Ubiquitin-independent proteolytic functions of the proteasome.* Archives of Biochemistry and Biophysics, 2003. **415**(12801506): p. 1-5.

30. Ampapathi, R.S., et al., *Order-disorder-order transitions mediate the activation of cholera toxin.* Journal of Molecular Biology, 2008. **377**(18272180): p. 748-60.

31. Elkabetz, Y., et al., *Distinct steps in dislocation of luminal endoplasmic reticulum-associated degradation substrates: roles of endoplamic reticulum-bound p97/Cdc48p and proteasome.* J Biol Chem, 2004. **279**(6): p. 3980-9.

32. Bar-Nun, S., *The role of p97/Cdc48p in endoplasmic reticulum-associated degradation: from the immune system to yeast.* Curr Top Microbiol Immunol, 2005. **300**: p. 95-125.

33. Kothe, M., et al., *Role of p97 AAA-ATPase in the retrotranslocation of the cholera toxin A1 chain, a non-ubiquitinated substrate.* J Biol Chem, 2005. **280**(30): p. 28127-32.

34. McConnell, E., A. Lass, and C. Wojcik, *Ufd1-Npl4 is a negative regulator of cholera toxin retrotranslocation.* Biochemical and Biophysical Research Communications, 2007. **355**(4): p. 1087-90.

35. Sreedhar, A.S., et al., *Hsp90 isoforms: functions, expression and clinical importance.* FEBS letters, 2004. **562**(15069952): p. 11-5.

36. Csermely, P., et al., *The 90-kDa Molecular Chaperone Family:: Structure, Function, and Clinical Applications. A Comprehensive Review.* Pharmacology & Therapeutics, 1998. **79**(15218328488919176698related:-hU8aSFdMtMJ): p. 129-168.

37. Taylor, M., et al., *Hsp90 is required for transfer of the cholera toxin A1 subunit from the endoplasmic reticulum to the cytosol.* The Journal of Biological Chemistry, 2010. **285**(20667832): p. 31261-7.

38. Bernardi, K.M., et al., *Derlin-1 facilitates the retro-translocation of cholera toxin.* Molecular Biology of the Cell, 2008. **19**(18094046): p. 877-84.

39. Dixit, G., et al., *Cholera Toxin Up-Regulates Endoplasmic Reticulum Proteins That Correlate with Sensitivity to the Toxin.* Experimental Biology and Medicine, 2008. **233**(2): p. 163-175.

40. Saslowsky, D.E., et al., *Intoxication of zebrafish and mammalian cells by cholera toxin depends on the flotillin/reggie proteins but not Derlin-1 or -2.* J Clin Invest, 2010. **120**(12): p. 4399-4409.

41. Ostrom, R.S. and P.A. Insel, *The evolving role of lipid rafts and caveolae in G protein-coupled receptor signaling: implications for molecular pharmacology.* British Journal of Pharmacology, 2004. **143**(2): p. 235-45.

42. Allen, J.A., R.A. Halverson-Tamboli, and M.M. Rasenick, *Lipid raft microdomains and neurotransmitter signalling.* Nat Rev Neurosci, 2007. **8**(2): p. 128-40.

43. Oh, P. and J.E. Schnitzer, *Segregation of heterotrimeric G proteins in cell surface microdomains. G(q) binds caveolin to concentrate in caveolae, whereas G(i) and G(s) target lipid rafts by default.* Mol Biol Cell, 2001. **12**(3): p. 685-98.

44. Ohkubo, S. and N. Nakahata, *[Role of lipid rafts in trimeric G protein-mediated signal transduction]*. Yakugaku Zasshi, 2007. **127**(1): p. 27-40.

45. Kamata, K., et al., *Functional evidence for presence of lipid rafts in erythrocyte membranes: Gsalpha in rafts is essential for signal transduction.* Am J Hematol, 2008. **83**(5): p. 371-5.

46. Ray, S., et al., *Lipid rafts alter the stability and activity of the cholera toxin A1 subunit.* J Biol Chem, 2012. **287**(36): p. 30395-405.

47. Murayama, T., et al., *Effects of temperature on ADP-ribosylation factor stimulation of cholera toxin activity.* Biochemistry, 1993. **32**(8422366): p. 561-6.

48. Tatulian, S.A., *Structural characterization of membrane proteins and peptides by FTIR and ATR-FTIR spectroscopy.* Methods in Molecular Biology, 2013. **974**: p. 177-218.

49. O'Neal, C.J., et al., *Crystal structures of an intrinsically active cholera toxin mutant yield insight into the toxin activation mechanism.* Biochemistry, 2004. **43**(15049684): p. 3772-82.

50. Winkeler, A., et al., *BiP-dependent export of cholera toxin from endoplasmic reticulum-derived microsomes.* FEBS letters, 2003. **554**(14623108): p. 439-42.

51. Schasfoort, R.B.M. and A.J. Tudos, *Handbook of surface plasmon resonance / editors, Richard B.M. Schasfoort and Anna J. Tudos*. 2008: Cambridge : Royal Society of Chemistry, 2008.

52. Ozdemir, S., Turhan-Sayan, G, *Temperature effects on surface plasmon resonance: Design considerations for an optical temperature sensor.* JOURNAL OF LIGHTWAVE TECHNOLOGY, 2003. **21**(3): p. 805-814.

53. Wagner, B.J. and J.W. Margolis, *Age-dependent association of isolated bovine lens multicatalytic proteinase complex (proteasome) with heat-shock protein 90, an endogenous inhibitor.* Arch Biochem Biophys, 1995. **323**(2): p. 455-62.

54. Tsubuki, S., Y. Saito, and S. Kawashima, *Purification and characterization of an endogenous inhibitor specific to the Z-Leu-Leu-Leu-MCA degrading activity in proteasome and its identification as heat-shock protein 90.* FEBS Lett, 1994. **344**(2-3): p. 229-33.

55. Whitesell, L., et al., *Inhibition of heat shock protein HSP90-pp60v-src heteroprotein complex formation by benzoquinone ansamycins: essential role for stress proteins in oncogenic transformation.* Proc Natl Acad Sci U S A, 1994. **91**(18): p. 8324-8.

56. Teter, K., M.G. Jobling, and R.K. Holmes, *Vesicular transport is not required for the cytoplasmic pool of cholera toxin to interact with the stimulatory alpha subunit of the heterotrimeric g protein.* Infection and Immunity, 2004. **72**(15557603): p. 6826-35.

57. Ray, S., et al., *Lipid Rafts Alter the Stability and Activity of the Cholera Toxin A1 Subunit.* J Biol Chem, 2012.

58. Giodini, A. and P. Cresswell, *Hsp90-mediated cytosolic refolding of exogenous proteins internalized by dendritic cells.* The EMBO journal, 2008. **27**(18046456): p. 201-11.

59. Minami, Y. and M. Minami, *Hsc70/Hsp40 chaperone system mediates the Hsp90-dependent refolding of firefly luciferase.* Genes to cells : devoted to molecular & cellular mechanisms, 1999. **4**(10620017): p. 721-9.

60. Zuehlke, A. and J.L. Johnson, *Hsp90 and co-chaperones twist the functions of diverse client proteins.* Biopolymers, 2010. **93**(3): p. 211-7.

61. Cintron, N.S. and D. Toft, *Defining the requirements for Hsp40 and Hsp70 in the Hsp90 chaperone pathway.* The Journal of Biological Chemistry, 2006. **281**(16854979): p. 26235-44.

62. Minami, Y., et al., *Regulation of the heat-shock protein 70 reaction cycle by the mammalian DnaJ homolog, Hsp40.* The Journal of Biological Chemistry, 1996. **271**(8702658): p. 19617-24.

63. Chen, S. and D.F. Smith, *Hop as an adaptor in the heat shock protein 70 (Hsp70) and hsp90 chaperone machinery.* The Journal of Biological Chemistry, 1998. **273**(9857057): p. 35194-200.

64. Carrigan, P.E., et al., *Domain:domain interactions within Hop, the Hsp70/Hsp90 organizing protein, are required for protein stability and structure.* Protein science : a publication of the Protein Society, 2006. **15**(16452615): p. 522-32.

65. Rajapandi, T., L.E. Greene, and E. Eisenberg, *The molecular chaperones Hsp90 and Hsc70 are both necessary and sufficient to activate hormone binding by glucocorticoid receptor.* The Journal of Biological Chemistry, 2000. **275**(10781595): p. 22597-604.

66. Jiang, J., et al., *Structural basis of J cochaperone binding and regulation of Hsp70.* Molecular cell, 2007. **28**(17996706): p. 422-33.

67. Mayer, M.P., *Gymnastics of molecular chaperones.* Mol Cell, 2010. **39**(3): p. 321-31.

68. Takeda, S. and D.B. McKay, *Kinetics of peptide binding to the bovine 70 kDa heat shock cognate protein, a molecular chaperone.* Biochemistry, 1996. **35**(8605215): p. 4636-44.

69. Chang, T.C., et al., *The effect of mutating arginine-469 on the substrate binding and refolding activities of 70-kDa heat shock cognate protein.* Archives of Biochemistry and Biophysics, 2001. **386**(11360998): p. 30-6.

70. Tyedmers, J., et al., *Assembly of heterodimeric luciferase after de novo synthesis of subunits in rabbit reticulocyte lysate involves hsc70 and hsp40 at a post-translational stage.* European Journal of Biochemistry / FEBS, 2000. **267**(10848974): p. 3575-82.

71. Taipale, M., D.F. Jarosz, and S. Lindquist, *HSP90 at the hub of protein homeostasis: emerging mechanistic insights.* Nat Rev Mol Cell Biol, 2010. **11**(7): p. 515-28.

72. Morishima, Y., et al., *The Hsp organizer protein hop enhances the rate of but is not essential for glucocorticoid receptor folding by the multiprotein Hsp90-based chaperone system.* J Biol Chem, 2000. **275**(10): p. 6894-900.

73. Hernandez, M.P., W.P. Sullivan, and D.O. Toft, *The assembly and intermolecular properties of the hsp70-Hop-hsp90 molecular chaperone complex.* The Journal of Biological Chemistry, 2002. **277**(12161444): p. 38294-304.

74. Murphy, P.J., et al., *Stoichiometry, abundance, and functional significance of the hsp90/hsp70-based multiprotein chaperone machinery in reticulocyte lysate.* J Biol Chem, 2001. **276**(32): p. 30092-8.